Novel control algorithm for MPPT with Boost converters in photovoltaic systems

Josean Ramos-Hernanz [a,*], *Jose Manuel Lopez-Guede* [b], *Oscar Barambones* [b], *Ekaitz Zulueta* [b], *Unai Fernandez-Gamiz* [c]

[a] *Electrical Engineering Department, Faculty of Engineering Vitoria-Gasteiz (University of the Basque Country, UPV/EHU), Vitoria-Gasteiz, Spain*
[b] *Systems Engineering and Automatic Department, Faculty of Engineering Vitoria-Gasteiz (University of the Basque Country, UPV/EHU), Vitoria-Gasteiz, Spain*
[c] *Nuclear Engineering and Fluid Mechanics Department, Faculty of Engineering Vitoria-Gasteiz (University of the Basque Country, UPV/EHU), Vitoria-Gasteiz, Spain*

a b s t r a c t

The great advances in efficiency and performance of photovoltaic modules would not be very useful if they do not work close to their maximum power point (MPP). In this paper a novel Sliding Mode Control (SMC) based algorithm is proposed to be implemented in a DC/DC converter in order to make an autonomous photovoltaic system to work at the MPP. Once that the design of the novel algorithm has been detailed (especially the novel part relative to the current reference signal) and its stability has been demonstrated, its performance has been compared with two of the most commonly used algorithms in this scope, i.e., Perturbation & Observation (P&O) and Incremental Conductance (IC) algorithms, in addition to a PI controller because it is one of the preferred controllers in industrial applications. This comparison has been carried out taking into account both simulated and experimental tests. The first focused on their behavior when sudden changes in irradiance and temperature, while the lasts analyzed them when the load resistance was varying arbitrarily in actual facilities (composed of a photovoltaic module Mitsubishi PV-TD185MF5, a Boost converter, a variable load and a real-time data acquisition card dSPACE DSP1104 used as the interface between the control algorithm implemented in Simulink/Matlab and the real photovoltaic module). After completing tests under different conditions, we found that the proposed SMC based algorithm outperforms the PI controller and the P&O and IC algorithms, especially in experiments carried out using actual facilities.

Introduction

Photovoltaic industry continues showing a steady and sustained growth worldwide. This is possible thanks to the fast cost reduction and to the increased efficiency of commercial photovoltaic modules. The world photovoltaic market has grown in recent years around 20% approximately. The dynamics of prices of modules and other basic components of the facilities has followed a descending trend since 2010, and

the same trend is continuing nowadays. This circumstance is allowing photovoltaic energy to become one of the best alternatives to deal with the growing demand for energy. One of its advantages is to mitigate the rising concern about CO_2 emissions and global warming. The null pollution of this energy processing makes it very interesting for facilities within cities [15], avoiding emissions from primary energy resources. During operation of an actual photovoltaic system, i.e., non-experimental or carried out in a laboratory, there are some variables on which it is difficult to influence, such as real irradiance or temperature because these variables are imposed by the weather conditions that exist at that time. However, there are variables on which it will be easier to act in order to vary the operation of photovoltaic module and make it to work in a more controlled situation, such as the output resistance at the photovoltaic module (R_{PV}). In order to achieve the purpose of keeping the PV module at a specific working point, it is mandatory to design a suitable converter.

The characteristic curves are one of the best suited tools to analyze the behavior of photovoltaic modules. There are three types of these curves: Current**e**Voltage (I**e**V), Power-Voltage (P**e**V) and Power-Current (P**e**I). Obviously, I**e**V curve shows the values of the points (V, I), and the same is applied to the remaining curves. Regarding their construction, there are two possibilities: on one hand, they could be the result of mathematical expressions that describe the behavior of the photovoltaic module at constant temperature and irradiance (as the manufacturers usually provide), and if the irradiance or temperature varies, the obtained curves will be different. On the other hand, it is possible to measure actual data from photovoltaic modules and draw the gathered data, probably with changing weather conditions (temperature and irradiance).

Usually, increased irradiance obtains more current and power, while increased temperature implies a decrease of current and power. Fig. 1 shows the characteristic curves I**e**V (black), P**e**V (blue), and P**e**I (magenta) of a photovoltaic module obtained at a given temperature and irradiance. The bottom horizontal axis represents the working voltage (V) of the photovoltaic module, while the above one represents the obtained current (A), which is also on the ordinate axis on the left side. Finally, the power output (W) is on the right ordinate axis.

The improvement of the performance of DC/DC converters used in photovoltaic systems is a very relevant topic for the academia [17,24], being the chosen algorithm for its control a key election for the operation of the converter in order to track the maximum power point depicted in Fig. 1. In this paper the chosen algorithm is the sliding mode control (SMC), due to the number of advantages which it involves [3,16]. This algorithm is one of the most widely used in many fields like Robotics [5] or in photovoltaic energy field [34] because of its high performance, robustness and simplicity of implementation. We have studied this algorithm from both simulation and experimentation point of view, while other authors study the control algorithms to analyze their behavior only from the simulation point of view [9,23,24,27].

Two of the most commonly used control algorithms by the researchers up to date for this purpose are the Perturbation and Observation (P&O) [31,33] and the Incremental Conductance (IC) algorithms [21,28]. Some authors usually compare their new algorithms with one of them [10,30], while other authors make the comparison between them [14,7]. For example, in Ref. [8] a new algorithm is proposed and compared with both P&O and IC algorithms. The process followed in this work is very similar: a novel control algorithm is developed for a DC/DC converter and it is compared with these two standard algorithms. In addition, we have also validated experimentally the results.

The PI controller is generally preferred in industrial applications due to its efficiency, simplicity and low cost [32]. The basic term is the proportional one (P), which generates a corrective control action proportional to the error. The integral term (I) generates a correction that is proportional to the integral of the error. This ensures that if a sufficient control effort is applied, the tracking error is reduced to zero [6].

There are some authors who mix different types of control algorithms. In Ref. [12] two controllers are proposed: a Fuzzy-PI controller for three-phase VSI of Proton Exchange Membrane Fuel Cell, and a Fuzzy-PI controller in companion with a small supercapacitor for three-phase VSI of Solid Oxide Fuel

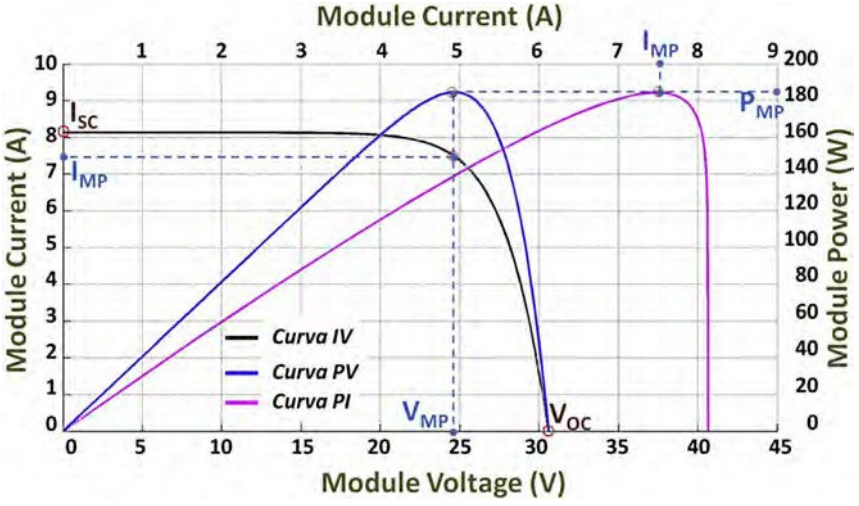

Fig. 1 **e** Characteristic curves of a photovoltaic module.

Cell DG. Numerical results demonstrate the efficacy of the proposed controller in comparison with PI controller for both Distributed Generations. On the other hand, in Ref. [22] the proposed converter consists of two cascade stages non isolated DC/DC converters. The control of the converters is ensured by a dual loop control that contains for the first stage a voltage loop with a linear PI controller and a fast-current loop using a non-linear sliding controller for both converters.

Another method that can be used to improve the MPP tracking in photovoltaic systems is Fuzzy Logic Control (FLC) [1,2,29]. In these works, some fuzzy rules are proposed using an input error that is based on the increment of the power versus the increment of the current. In addition, in these works there is a demonstration of the stability of the system in closed loop. This method may be unsuitable if the current measurements contain noise and the system is in the segment of the I**e**V characteristic curve where the current values are practically constant. Another usual drawback of the FLC is the configuration and tuning of a high number of rules, which requires a large amount of operations on the plant [4].

In Ref. [10] the authors of this paper proposed a fuzzy controller with a single input (SIFLC) to track the MPP of a photovoltaic system. To achieve this, the voltage produced by the photovoltaic module is compared with the reference voltage that the photovoltaic system should have if it were working in the MPP and this error is taken as input from the FLC. The output of the FLC is responsible for continuously adjusting the duty cycle of the DC/DC converter, so that the photovoltaic system always works in the MPP.

The work was carried out in the same facilities and with the same devices used in this work, with the unique difference of the photovoltaic modules. The SIFLC systems do not present a high computational load because they usually have a lower number of rules and in addition these rules are usually simple, so that the calculation time of the control signal can be reduced [11]. This method has been applied, among others, to the control of a first order system with dead time, the control of orbital tracking of a system and the identification of nonlinear functions [13].

The control loop with a DC**e**DC converter and the photovoltaic module can be carried out through the interface shown in Fig. 2. The MPPT block contains the maximum power point tracking algorithm, which is responsible for generating the reference value I_{REF} (or V_{REF}) from the measurement of the current I_{PV} (or voltage V_{PV}) which is being provided at that moment by the photovoltaic module. The Controller Block (which generates the Duty Cycle d as shown in Fig. 2) receives the reference value I_{REF} (or V_{REF}) from the MPPT block corresponding to the value of the adequate current (or voltage) at which the photovoltaic module should work in order to obtain the maximum power. With this reference value and taking into account the load, the converter duty cycle (d) is modified.

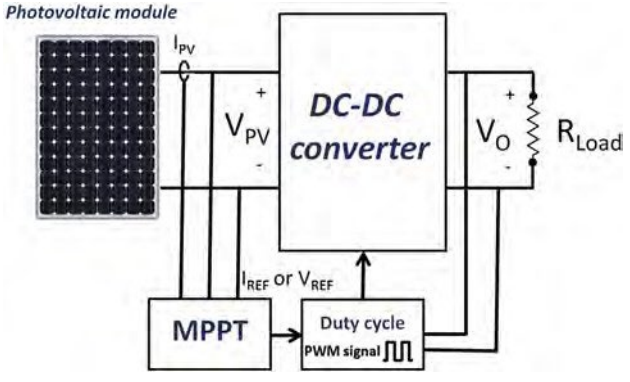

Fig. 2 **e** Control interface between DC**e**DC converter and photovoltaic module.

Our system consists of three main elements, i.e., the photovoltaic module, the DC/DC converter and a variable load. In this paper we include studies on some elements belonging to the autonomous photovoltaic system:

- Authors toke measures during 20 months with an approximate average of 10 min per each measurement process. These measures attempt to cover the largest possible number of different weather situations, so approximately 63,000 samples (with I_{PV}, V_{PV}, Temperature and Irradiance) were obtained. Using these data (sorted by temperatures and irradiances) characteristic curves P**e**I are generated and the maximum power point of each one of them is calculated.
- Four control algorithms are designed and implemented in Matlab/Simulink, i.e., Perturbation and Observation (P&O), Incremental Conductance (IC), PI controller and Sliding Mode Control (SMC). Their behaviors are simulated in two different experiments: the first one at constant irradiance and variable temperature, while the second one at constant temperature and variable irradiance.
- With the previously obtained data a reference current generator is designed to provide the control signal so that the DC/DC converter makes the photovoltaic module to work at the maximum power point, when the PI controller and SMC algorithm are used.
- And as last part of our work, we discuss the operation of the four control algorithms in the real photovoltaic installation that is on the roof of the Faculty of Engineering Vitoria-Gasteiz when have to deal with sudden changes in the value of the load resistance. This facility operates in real time with RTI Matlab/Simulink and the data acquisition card dSPACE DSP1104 for real validation of our results. This way of validation is appropriate due to its ease of use and the possibility of storing the results in real time [19,21 and 25].

The photovoltaic panel with which we have worked during both simulated and real tests is the Mitsubishi Electric PV-TD185MF5. In order to carry out the simulations we have used an artificial neural network based model developed by authors in Ref. [18], whose main characteristic is the precision predicting the electrical behavior of the photovoltaic module. To develop such model the main variables which influence the photovoltaic module have been taken into account, i.e., three input variables (Temperature, Irradiance and the output voltage of the photovoltaic module V_{PV}) and a single output variable (the current to the output of the photovoltaic module I_{PV}). This neural network was trained with the same data that have been used in the current generator of this paper, obtaining a root mean squared error (RMSE) accuracy of 0.042 A, i.e., larger than the accuracy of the measuring devices.

On the other hand, during the real experimental test of the P&O, IC, PI and the SMC based algorithm proposed in this paper, we found that the best results in order to MPP tracking by the photovoltaic module were reached by the last one.

The paper is structured as follows: in Section Background an overview of basic concepts used in this work is given (DC/DC Boost converters, a number of control algorithms as P&O, IC and SMC, the dSPACE DSP1104 controller card and the process of acquiring the necessary data for the design of reference current generator). Section Sliding mode control design describes the design of the sliding mode control based algorithm introduced in this paper and the modeling process of the reference current generator. Section Simulation results of the algorithms and Section Real world tests discuss both the simulated and the real experimental results respectively. Finally, our conclusions are given in Section Conclusion.

Background

This section gives a basic background on relevant topics for the scope of this paper. Besides, the last two subsections are devoted to partially explain the use of the DSP board that has been used for the real-world tests of the introduced algorithm, as well as the procedure that has been used to record the necessary data to obtain the characteristic curves of the photovoltaic panels.

Boost converter

DC/DC converters are switching systems that control the average value of the voltage (or current) at the output (load) varying the switching times between the input (DC source) and the output, allowing adjust the uncontrolled voltage supplied by the photovoltaic modules to a regulated DC voltage at its output.

Converters switching is carried out by semiconductor devices which are usually controlled through pulse width modulation (PWM), varying the nature of these "switches" depending on the power and frequency of the used operation.

This method has a constant switching time (T), which is defined as the sum of driving time (T_{ON}) and lock time (T_{OFF}). Varying the driving time (T_{ON}), it is possible to control the output average voltage.

The energy supplied to the load depends on the duty cycle (d), defined as the ratio between the time in which the converter is driving (T_{ON}) and the switching time ($T = T_{ON} + T_{OFF}$), i.e., $d = T_{ON}/T$.

DC/DC converters can operate in two different modes with respect to the current of the coil (IL). If this current never reaches the zero value, the converter will be working in Continuous Conduction Mode (CCM), while if the output current is low or the working frequency decreases, the coil current will be zero during part of the period working in the Discontinuous Conduction Mode (DCM). The CCM mode is preferred as a means to maximize the performance and operation of the semiconductors and passive components of the converter.

The converter chosen for the experimental part of the paper is of Boost type. In Fig. 3(a) we can see its typical topology. This type of converter has a higher output continuous voltage than the input voltage, while its output current is lower than the input one. The configuration of this type of converter is composed of at least two semiconductor switches, an energy storage element and an output filter. The order of the converter is determined by the number of energy storage elements that it contains.

This type of converter is a non-linear or variable-structure system, since the structure varies depending on the two states of the switch:

1) When the switch (S) is driving (T_{ON}), Fig. 3(b), the diode (D) is reverse biased isolating the input and output stages. The result is a voltage $V_L = V_S$ positive and constant in the coil (L), which makes the current through the coil (I_L) grow linearly. In this state, all the voltage is applied to the coil, therefore the power supplied by the photovoltaic modules is stored in the coil (L) while the capacitor (C) transfers its energy to the load.
2) When the switch (S) is opened (T_{OFF}), it does not conduct as shown in Fig. 3(c), so the diode (D) is polarized in direct mode and the output stage is connected to the input one. The

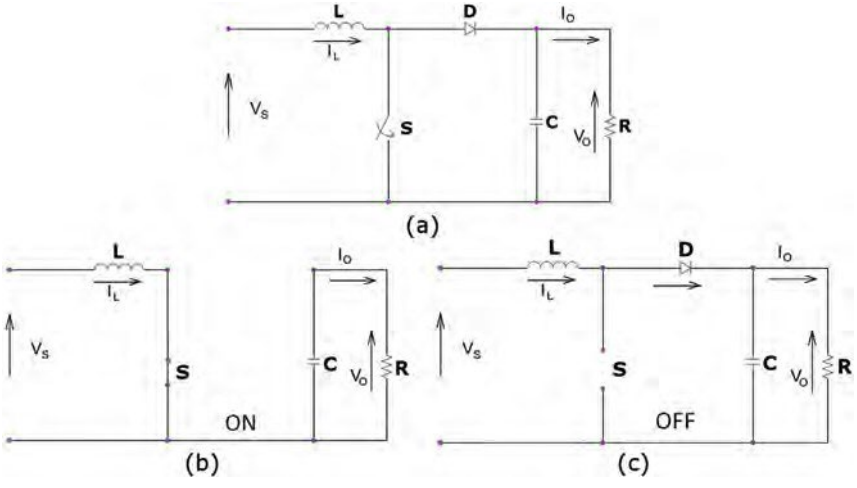

Fig. 3 – Boost DC–DC converter topology and working modes.

voltage of the coil (L) is added to the voltage of the photovoltaic modules obtaining in this way always an output voltage higher than of the source and of same polarity. The energy supplied by the photovoltaic modules is transferred to the load through the coil (L) and of the diode (D). In this state, the voltage of the coil is $V_L = V_S - V_O$. As we have stated, this is a Boost converter $V_O > V_S$, so the intensity decreases linearly following the slope $m = (V_S - V_O)/L$.

As it a matter of fact that during a complete cycle the voltage at the terminals of an inductor is zero, we can state that the volts-second received are equal to the volts-second delivered so that the total volts-second that the inductor receives in a switching period are given by Eq. (1):

$$\int_0^T V_L dt = V_S dT + (V_S - V_O)(1 - d)T \tag{1}$$

If we set to zero and solve the equation, we obtain Eq. (2) relating the output voltage to the input voltage [20]:

$$V_S - V_O(1 - d) = 0 \tag{2}$$

$$V_O = \frac{V_S}{(1 - d)} \tag{3}$$

In Eq. (3) it is demonstrated that the output voltage is greater than the input for $0 < d < 1$, and that the output voltage at the load is proportional to the duty cycle (d) for a given supply voltage.

Assuming no losses in the circuit elements, the power supplied by the photovoltaic module should be equal to the power delivered to the load as expressed in Eq. (4):

$$P_S = P_O = V_S I_S = V_O I_O \tag{4}$$

Substituting Eq. (4) in Eq. (3) we obtain:

$$I_O = I_S(1 - d) \tag{5}$$

If we consider that the resistance of the load is $R = V_O/I_O$, it can be expressed by Eq. (6):

$$R_O = \frac{R_S}{(1 - d)^2} \tag{6}$$

This implies that the resistance from the point of view of the photovoltaic module it is directly proportional to the resistance R_S connected to the output of the converter and inversely to the square of the complement of the duty cycle (d), being its value within the range [0, R).

Analyzing Eqs. (3), (5) and (6), it can be seen that if $d \in (0, 1]$, the current is reduced because the converter voltage increases.

The dynamic model of the converter is determined by the two equations system given by Eq. (7) [25]:

$$\begin{aligned} L\frac{dI_L}{dt} &= -(1 - u)V_C + V_S \\ C\frac{dV_C}{dt} &= (1 - u)I_L - \frac{V_O}{R} \end{aligned} \tag{7}$$

being I_L the current through the coil and V_C the output voltage (equal to V_O) between the capacitor terminals. The control input u represents the switch position (S), which is a binary signal taking values in the set $u \in \{0, 1\}$, corresponding to the operating mode of the circuit when $u = 1$ (Fig. 3(b)) or when $u = 0$ (Fig. 3(c)). The system consists of the inductance L of the input circuit, the output filter capacitance C and the load resistance R at the output, taking into account that the voltage of the photovoltaic module takes the value V_S.

Making some rearrangements of the factors we obtain Eq. (8):

$$\begin{aligned} \frac{dI_L}{dt} &= \frac{V_S}{L} - \frac{1}{L}(1 - u)V_O \\ \frac{dV_O}{dt} &= \frac{1}{C}(I_L - I_O) - \frac{1}{C}uI_L \end{aligned} \tag{8}$$

It allows expressing the dynamics of system through Eqs. (9) and (10):

$$\dot{x} = f(x) + g(x)u \tag{9}$$

where:

$$x = \begin{bmatrix} I_L \\ V_O \end{bmatrix}$$

$$f(x) = \begin{bmatrix} \frac{V_S}{L} - \frac{V_O}{L} \\ \frac{1}{C}I_L - \frac{V_O}{RC} \end{bmatrix}$$

$$g(x) = \begin{bmatrix} \frac{V_O}{L} \\ -\frac{I_L}{C} \end{bmatrix} \tag{10}$$

Perturbation & Observation algorithm (P&O)

The Perturbation and Observation (P&O) algorithm is one of the most widely used for control of DC/DC converters, mainly due to its easy implementation since it has a simple structure and it requires to measure only few variables.

The main idea guiding the algorithm is that when the photovoltaic module is working at any non-MPP point, the operating voltage of the module is disturbed (varied) periodically (increased or decreased) in a small voltage V though the converter duty cycle. Then the change on the output power DP of the photovoltaic module is measured. If $DP > 0$, the operating point is closer to the MPP and the next disturbance will occur in the same direction as the previous one (with the same algebraic sign). However, if $DP < 0$, the system has moved away from MPP and the next disturbance will take place in the opposite direction (opposite algebraic sign). This disturbance is achieved by the unique variable to which the access control system has access, i.e., the duty cycle (d). An increment in the duty cycle (d) implies a decrement in input resistance of the DC/DC converter, and therefore a decrement in the operating voltage of the photovoltaic module (and vice versa). Once the MPP has been reached, the P&O algorithm makes the point of operation of the photovoltaic module to work around it. The disturbance could also be done on the photovoltaic module current instead of on voltage.

There are four possible situations in which the photovoltaic module can work and in the following paragraphs we will

analyze its behavior in order to track the MPP [31]. Actually, it is based on calculating the power and voltage increase on the I**e**V curve of the photovoltaic module of Fig. 4:

- DP ¼ P(k)−P(k−1)>0 and DV ¼ V(k)−V(k−1)>0

The power change at time k is denoted as DP and named power increase. This is the result of the current power minus the power at the previous sample, and in this case, it is positive. The second condition to fulfill is that the output DV (also defined as the difference between the existing voltage minus voltage at the previous sample) of the photovoltaic module is also positive. Given these two conditions, the algorithm will decrease the duty cycle (d) in such a way that the output voltage of the photovoltaic module continues to rise until reaching the MPP.

- DP ¼ P(k)−P(k−1)>0 and DV ¼ V(k)−V(k−1)<0

In this case the increase of power DP is positive while the increase of output voltage DV is negative. The control action to make in this situation is to increase the duty cycle (d) so that further decrements of the output voltage of the photovoltaic module will take place until the MPP is reached.

- DP ¼ P(k)−P(k−1)<0 and DV ¼ V(k)−V(k−1)<0

In this third case the increment of power DP and output voltage DV are negative. The control action to be performed in this case is to decrease the duty cycle (d) to increase the output voltage of the photovoltaic module until the MPP is reached.

- DP ¼ P(k)−P(k−1)<0 and DV ¼ V(k)−V(k−1)>0

In this last case, the increment of power DP is negative while the increment of output voltage DV is positive. The control action to perform in these circumstances is to increase the duty cycle (d) so that further decrements of the output voltage of the photovoltaic module continue until the MPP is reached.

The summary of the behavior of this algorithm is shown in Table 1.

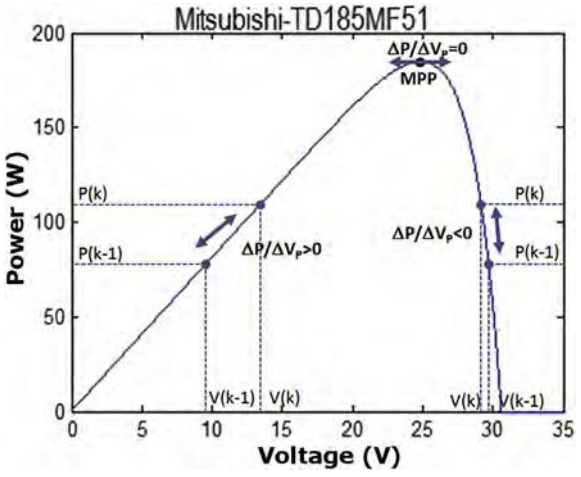

Fig. 4 **e** Evolution of the MPP tracking by P&O Algorithm.

Table 1 **e** Summary of the behavior of P&O Algorithm.

Measurements	Duty cycle (d)	Voltage
DP > 0 and DV > 0	Decrease	Increase
DP > 0 and DV < 0	Increase	Decrease
DP < 0 and DV > 0	Decrease	Increase
DP < 0 and DV < 0	Increase	Decrease

In Fig. 5 the flowchart of operation of this algorithm is shown, where I(k), V(k) and P(k) are the current, the voltage and the power of the photovoltaic module measures at time (k) [14]. I(k−1), V(k−1) and P(k−1) are the current, the voltage and the power of the photovoltaic module at the previous time (k−1). The algorithm compares the existing power with the previous one and based on this result it determines whether the same disturbance is still applied or its sign should be inverted at the next control cycle.

Its main drawback is that its efficiency depends on the speed updating the variable values, which will depend on the sampling frequency. A slow sampling can cause instability in the system to reach the MPP because the algorithm can sometimes take a lot of time to find the MPP and there would be significant energy looses. It cannot determine when it has exactly reached the MPP, so that it remains oscillating at the working point around the MPP. It also has errors in fast changing weather conditions because the algorithm does not perceive changes in the environmental conditions, for example, in partially cloudy days. The reason is that the algorithm does not difference between power variations due to variations caused by changes in the duty cycle or those caused by climate changes.

Incremental conductance algorithm (IC)

The electrical conductance (G) is the ease of a material to be crossed by an electric current, i.e., it is the inverse property of electrical resistance as Eq. (11) shows.

$$G = \frac{1}{R} = \frac{I}{V} \tag{11}$$

A higher conductance decreases the electrical resistance, and vice versa, so they are inversely proportional. It is denoted by the symbol G and is measured in Siemens (S).

Incremental Conductance (IC) algorithm is very similar to P&O algorithm. This algorithm is based on that the slope in the characteristic power-voltage (P**e**V) curve of the photovoltaic module is equal to zero at the MPP, i.e., the derivative of the output power of the photovoltaic module is equal to zero at that point. As shown in Fig. 6, the derivative is positive to the left and negative to the right of the MPP. Thus, the voltage of the photovoltaic module can be regulated close to the voltage value at the MPP tracking its incremental conductance (dI/dV) and its conductance (I/V).

This algorithm is based on the measurement of existing voltage and current (V_F and I_F) and on the voltage and current of the previous sample (V_I and I_I). Using them current increment is analyzed, i.e., dI ¼ I_F−I_I and the same concept is applied to the voltage (dV ¼ V_F−V_I). These parameters give the initial point to the algorithm and define the incremental

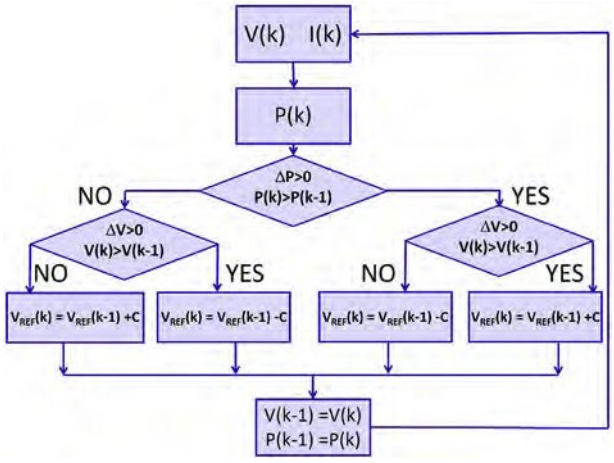

Fig. 5 **e** Flowchart of the P&O algorithm.

conductance as dI/dV. It is possible to express this idea through Eq. (12).

$$\frac{dP}{dV}\Big|_{MPP} = 0$$
$$\frac{dP}{dV} = \frac{d(I \cdot V)}{dV} = I + V\frac{dI}{dV} = 0 \Rightarrow I + V\frac{\Delta I}{\Delta V}$$
$$V\frac{dI}{dV} = -I \qquad (12)$$
$$\frac{dI}{dV} = -\frac{I}{V}$$

When these conditions are not met, the points around the maximum value are analyzed as follows [9]:

- dI/dV = **e**I/V, then dP/dV = 0; and the working point is at the MPP
- dI/dV > **e**I/V, then dP/dV > 0; and the working point is to the left of the MPP
- dI/dV < **e**I/V, then dP/dV < 0; and the working point is to the right of the MPP

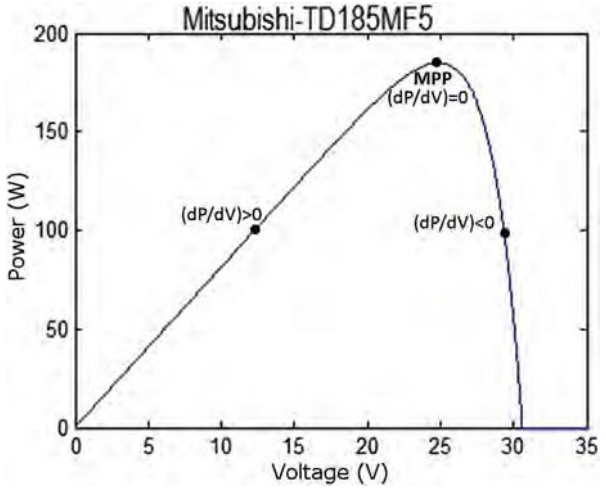

Fig. 6 **e** Evolution of the MPP tracking following the IC Algorithm.

The flowchart of Fig. 7 shows the MPP tracking algorithm to calculate it comparing the instantaneous conductance (I/V) and its increase. The voltage V_{Ref} value is the reference voltage to which the photovoltaic module is required to operate.

When the IC algorithm reaches the MPP, the voltage V_{REF} is equal to the voltage V_{MPP}. The photovoltaic module will continue operating at this point until there is a change in current, which will be due to variations in weather conditions, moment in which the algorithm will start again the search for the MPP. The summary of the behavior of this algorithm is shown in Table 2:

This algorithm has advantages such as its high precision reaching the MPP, little swing around the MPP and higher efficiency to deal with changes and disturbances generated by environmental conditions. The main advantage of the IC algorithm over the P&O algorithm is that it can calculate at any time the direction in which to change the operating point of the photovoltaic generator to take it closer to the MPP, and it can also determine when it has been reached. That is why under fast weather changes it will not take the wrong direction and in addition, once the MPP has been reached, the working point does not oscillate around it.

However, its main disadvantage that this algorithm has a more complex design. A quick MPP tracking can be achieved if large changes of the operating point are carried out increasing the size of the duty cycle (d), but we could make the system to work at points away from the MPP. On the other hand, if such variations are small, the algorithm can work closer to the MPP but the variations due to weather changes will be slower. So, it is mandatory to reach a balance between speed and accuracy.

Sliding mode control (SMC)

In this subsection, we recall the basics of sliding mode control (SMC), and its specific utilization will be explained later in the appropriate section of the paper.

SMC is defined as the control strategy that assigns a control signal to the converter that switches at high frequency and takes the system state to a scalar field S(x) named sliding surface. This surface is designed to meet the desired specifications and it could be any function of the state x that reduces

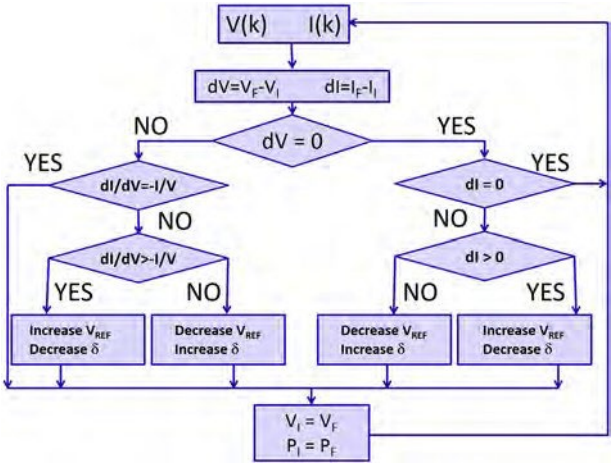

Fig. 7 **e** Flowchart of the MPPT IC algorithm.

Table 2 – Summary of the behavior of the IC Algorithm.

Measurements	Duty cycle (d)	Voltage
dV = 0 and dI/dV = −I/V	Keep	Keep
dV = 0 and dI/dV > −I/V	Decrease	Increase
dP/dV > 0		
dV = 0 and dI/dV < −I/V	Increase	Decrease
dP/dV < 0		
dV = 0 and dI = 0	Keep	Keep
dV = 0 and dI > 0	Decrease	Increase
dV = 0 and dI < 0	Increase	Decrease

to zero the regulation or tracking error in steady state. When the trajectory of the system evolves over the surface, it is said that the system is in sliding mode.

Focusing in our specific case, the used Boost Converter is a system with a single control input, linear with respect to the control signal and can be defined in the following way:

$$\dot{x} = f(x) + g(x)u \qquad x \in \mathbb{R}^n \quad u \in \mathbb{R} \tag{13}$$

where x is its state vector and the functions f and g are two smooth vector fields with $g(x) \neq 0$ for all x, and u is the discontinuous control signal taking the values zero or one. The discontinuities are corresponding to the changes of behavior of the converter, so converters are variable structure systems.

We have the control law or variable structure switching logic of Eq. (14), which makes the control action (u) to take one of the two feasible values depending on whether the reference current is higher or lower than the current at the output of the photovoltaic module.

$$u = \begin{cases} 1 & \text{for } s(x) > 0 \\ 0 & \text{for } s(x) < 0 \end{cases} \tag{14}$$

Under the action of the control law of Eq. (14), the balance point of the substructure corresponding to $u = 1$ is located in the region corresponding to $u = 0$, so the system state trajectory crosses the line of sliding and vice versa.

The function $s(x)$ is called switching function and determines the surface of dimension (n−1) given by Eq. (15).

$$S = \{x \in \mathbb{R}^n : s(x) = 0\} \tag{15}$$

The surface S is called discontinuity surface or switching surface, and it is any function of the state x that reduces to zero the regulation error or the steady state tracking. In this case, the surfaces correspond to changes of the converter structure. We say that the converter is controlled in sliding mode when the used control law is described by Eq. (14).

The switching function $s(x)$ and its time derivative must have opposite signs in order to make the trajectories to tend towards S. The conditions of existence of sliding mode can be expressed by Eq. (16):

$$\begin{aligned} &\frac{ds}{dt} < 0 \quad \text{for } s(x) > 0 \\ &\frac{ds}{dt} > 0 \quad \text{for } s(x) < 0 \end{aligned} \tag{16}$$

When the system is out of the surface, the movement of the system with respect to time $dS(x)/dt$ is directed towards the surface. A sliding region is the set of points of S, where Eq. (16) is satisfied.

dSPACE DSP1104 R&D controller board

Digital signal processors (DSP) in real time (for example, the device dSPACE DSP1104) are widely used in industry and research because they allow reducing the time between simulation and development of the real model. dSPACE DSP1104 controller board allows the development of multivariable high-speed digital controllers and prototyping in real time [25].

The DSP1104 has a main processor MPC8240 (PowerPC 603e core at 250 MHz), with an internal cache of 32 Kbytes and a slave DSP subsystem DSP TMS320F240 of the Texas Instruments company.

The working process is as follows:

1) Create a Simulink model with the control strategies using basic blocks or toolboxes. The process to create the model is the same than to create any Simulink scheme, but it is mandatory to install the library RTI1104.
2) Compile the model and generate specific code for real-time dSPACE (Tools>Code Generation>Build Model in Simulink).
3) Generate the interface using simple elements of the graphical user interface (GUI) as buttons, displays, radio buttons, etc. or even more elements as plotters, photo-realism, etc. in the ControlDesk 5.1 software, as shown in Fig. 8, specifying which is file contains the real-time code obtained from the compilation in Simulink.
4) Enable real-time process that allows displaying, handling and recording system variables in real time through the screen and graphical user interface.

Data acquisition

In order to model the reference current generator (part of the SMC based algorithm proposed in this paper) authors have used experimental data acquired from measurements made from the Mitsubishi PV-TD185-MF5 photovoltaic modules that are placed on the roof of the Faculty of Engineering Vitoria-Gasteiz (Spain). The model is made from experimental data, approximately 63,000 samples obtained during more than twenty months. These measurements are made in an arbitrary fashion with an average duration of 10 min. Each sample is composed of four variables: temperature, irradiance, intensity supplied by the module (I_{PV}) and the voltage between the output terminals of the module (V_{PV}) for different values of load resistance.

In Fig. 9 a scheme with the arrangement of the devices involved in the capturing process of raw data (T, G, V_{PV} and I_{PV}) is shown. Modifying the variable resistance authors varied the load value obtaining different pairs of voltage–current points for the irradiance and temperature that was at that time according to the weather conditions.

The measuring elements that have been used in the experimental part of the paper are the following:

- Irradiance and Temperature Sensor (Si-420TC-T-K): This element is a pattern cell that is composed of a monocrystalline solar cell (50 × 33 mm) and a temperature

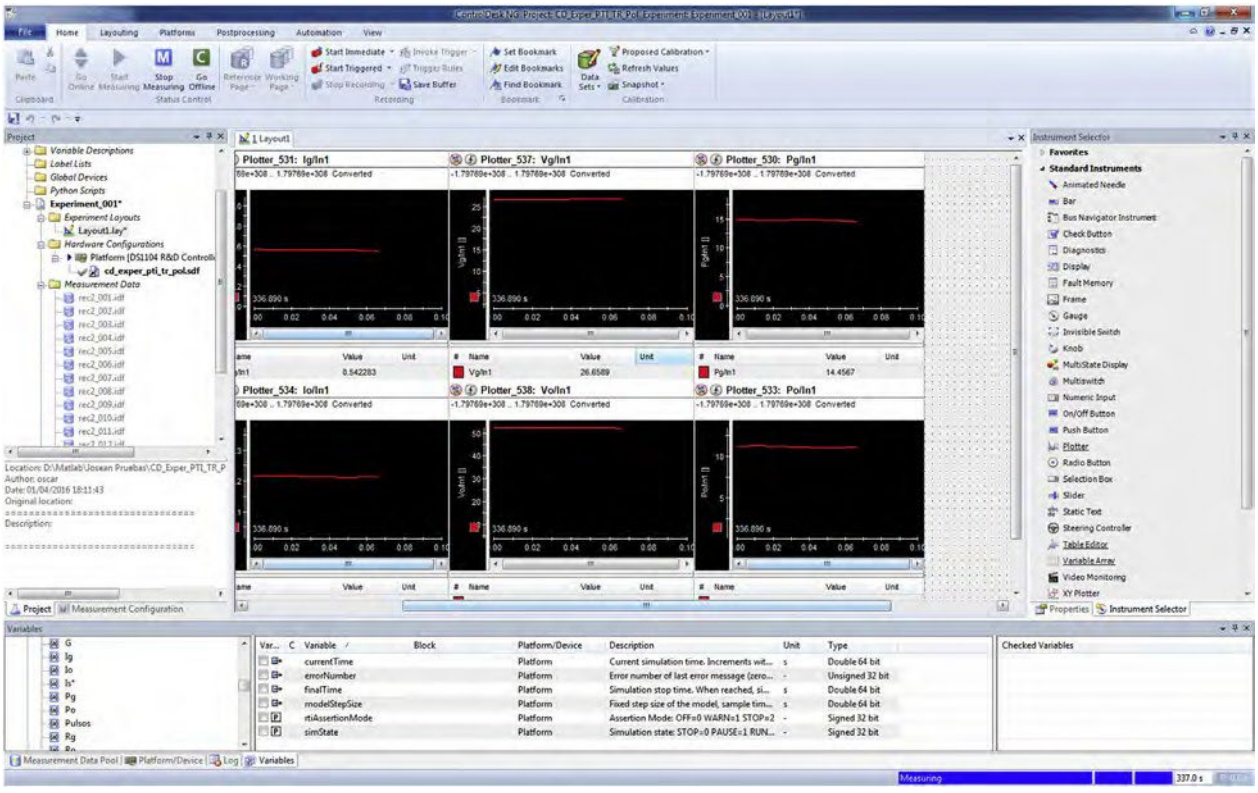

Fig. 8 ● Screenshot of the ControlDesk 5.1 software.

sensor (from −20 to 70 ° C). It provides the values of irradiance (W/m²) and temperature (° C) in the place of the photovoltaic modules during the data acquisition process. The accuracy of the device is ±5% when the irradiance is measured and ±1.5 ° C when dealing with temperature.

- Clamp Current Chauvin Arnoux PAC 12: This current clamp allows measuring the direct current supplied by the photovoltaic module without opening the circuit. The scale of work ranges from 0.4 to 60 A in direct current, with an accuracy of ±1.5%. The value of the maximum error is approximately ±150 mA. This device provides a voltage proportional to the direct current measured. Therefore, we need another element (TV809) that converts the measured voltage to its current proportional value.

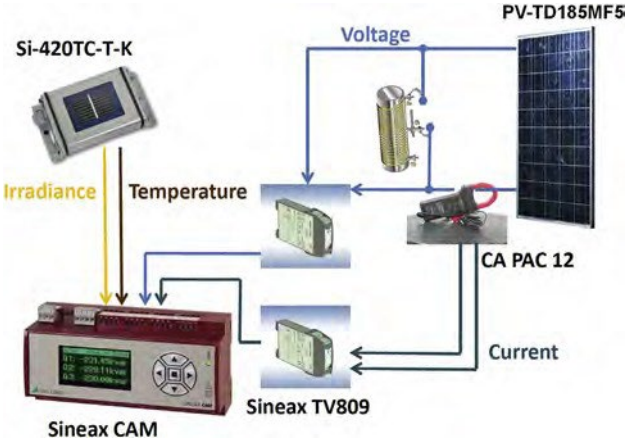

Fig. 9 ● Scheme of measurement elements for data logging.

- Programmable Amplifier with Insulation SINEAX TV809: The function of this device is to isolate electrically signals of input/output and amplify/convert the level of the input direct current signal from current to voltage or vice versa, using its configuration set up with a personal computer using the TV800plus V1.11 software. Since both the voltage of the photovoltaic module and the measured current are provided in volts, two TV809 devices are needed to convert these tensions to a proportional current (4●20 mA). It is due to the fact that the used data logger (SINEAX CAM) supports only measures provided in values of current. The accuracy of this device is ±0.2% of the maximum value of the input.
- SINEAX CAM Data Logger: This device is designed to make long-term measurements in industrial installations or electrical distribution networks. It allows a continuous measurement and its recording. The I/O interface can be arbitrarily configured. In our case, the parameters selected for recording are irradiance, temperature, voltage and current. The configuration of the device is quick and easy using the CB-Manager software. The CB-Manager takes a measurement every 2 s. The accuracy of this device is ±0.1% of the maximum value of the input configuration that is 20 mA, so the measurement error is negligible.

Sliding mode control design

This section is devoted to describe the sliding mode control (SMC) based algorithm which is introduced in this paper.

As was explained in Subsection Sliding mode control (SMC), the function of the SMC is to calculate a reference current to be compared with the current that is provided by the photovoltaic module and then to generate the value of the duty cycle (d), so that the photovoltaic module works in MPP.

In order to obtain the reference current, we have used the P**e**I characteristic curves provided by the acquired experimental data following the procedure explained in Subsection Data acquisition. Knowing these curves, we know their points of maximum power, and with them we can form different straight lines for each temperature, in such a way that with them, we create a plane that will give the value of the reference current at any power and temperature value.

Reference current generator

The reference signal generator has been designed using data obtained from real experimental measurements. The data acquisition process was explained in Subsection Data acquisition.

For modeling the generator of reference current I_{REF} we rely on the characteristic curve P**e**I. We can see the P**e**I curves corresponding to a number of irradiances ranging from 100 to 1000 W/m² in Fig. 10. In each one of them, its maximum power point (MPP) is marked through a red circle, in such a way that the values of the maximum power points form straight line in blue instead of a parable that would be the result if we would use the P**e**V characteristic curve. Once that this line is obtained, it is possible to know which is the value of the current at the maximum power point, i.e., the necessary reference current, for any power at which the photovoltaic module is working. Given that the power generated by the module depends on the temperature, it is mandatory to obtain all straight lines for the different values of temperature at which it can work.

Experimental reference current generator

The obtained data were divided into groups characterized by a temperature amplitude of 5 °C, from 5 °C to 50 °C. The data of these groups are divided again into groups paying attention to their irradiance values, from 100 to 1000 W/m², with a step of 25 W/m².

We have taken the data regarding current and power samples and using the tool *cftool* of Matlab, we got an equation which defines the P**e**I characteristic curve for each irradiance. In this way, we got a group of P**e**I curves corresponding to different irradiances for each temperature. From these equations-curves it is possible to obtain their maximum power points in order to get a set of straight lines similar to the blue line shown in Fig. 10 for each temperature. To illustrate the obtained results, Fig. 11 shows the different straight lines obtained for the groups of temperatures corresponding to 5 °C, 15 °C, 25 °C, 35 °C and 45 °C.

For each temperature we obtained a straight line $I_{MPP} = f(P_{MPP})$ in such a way that we found an equation that relates power and intensity of the maximum power points for each group of temperatures. Using these equations, we obtained sample vectors containing (P_{MPP}, T, I_{MPP}), which relate the value of the current in the MPP with given values of power and temperature in MPP.

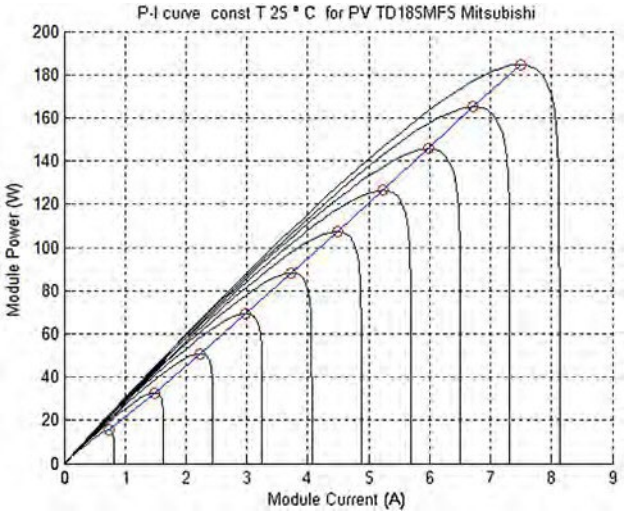

Fig. 10 **e** P-I characteristic curves of the module at different irradiance conditions.

From these (P_{MPP}, T, I_{MPP}) data and using the tool *cftool* of Matlab, a surface that gives the reference current from P_{MPP} and T, ($I_{MPP} = f(P_{MPP}, T)$) is obtained, as shown in Fig. 12. Knowing the power generated by the photovoltaic module and the operating temperature, the surface gives the reference current (I_{REF}), i.e., the current in the MPP (I_{MPP}). In this way, it is not necessary to know the value of the irradiance to get the values of the maximum power points.

In order to obtain the function of $I_{MPP} = f(P_{MPP}, T)$, different methods such as polynomial equations, Fourier, Gauss, etc. were used. Using for the curve fitting tool of Matlab, i.e., *cftool*, the function that best fits all the points of maximum power and temperature was polynomial function defined as shown in Fig. 13.

Stability demonstration

The designed converter should regulate its output current (I_O) at a reference value (I_{REF}). We have a control law in the same

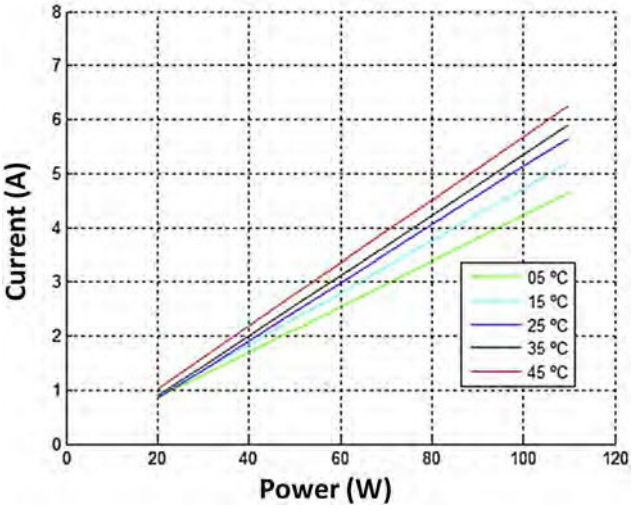

Fig. 11 **e** Lines of MPP for different temperatures (°C).

way as Eq. (14) with the following switching function [26] of Eq. (17).

$$S = I_{REF} - I_{PV} \tag{17}$$

The corresponding switching surface is defined by Eq. (18) as follows:

$$S = f(x) = I_{REF} = I_{PV} \tag{18}$$

being S a sliding region and the trajectory that reaches is the same sliding surface. An ideal regulation of system has been achieved because from now on it will evolve in sliding mode achieving always that $I_{REF} = I_{PV}$.

The polynomial calculated in the previous subsection gives the reference currents required by the system at all times. Using that value, the converter makes the photovoltaic module to follow it and to work in the area of the maximum power.

We define the switching function and the control law of Eq. (19) [26]:

$$u = \begin{cases} 1 & S > 0 \\ 0 & S < 0 \end{cases} \quad S = e = I_{REF} - I_{PV} \tag{19}$$

If S is a sliding region and the trajectory reaches the sliding surface, then a system ideal regulation has been achieved because from that moment it will evolve in sliding mode ensuring that always $I_{REF} = I_{PV}$. For best performance is behavior of the control signal of the proposed DC/DC converter, the integral of the control signal works in a range between 0.1 and 0.9.

The demonstration of the stability of the proposed controller is based on the theory of Lyapunov stability, so the following Lyapunov function is defined by Eq. (20):

$$V = \frac{1}{2} S^2 > 0 \tag{20}$$

The derivative with respect to time of this function is given by Eq. (21):

$$\dot{V} = S\frac{dS}{dt} \quad S\dot{S} < 0 \tag{21}$$

Adjusting Eq. (19) to our switching function we obtain Eq. (22):

```
f(x,y) = p00 + p10*x + p01*y + p20*x2 +
p11*x*y

Coefficients (with 95% confidence bounds):
    p00 = -0.04808 (-0.1204, 0.02424)
    p10 = 0.04275 (0.04102, 0.04448)
    p01 = -0.005689 (-0.007506, -0.003872)
    p20 = -1.833e-19 (-1.177e-05, 1.177e-05)
    p11 = 0.0004055 (0.0003791, 0.0004319)

Goodness of fit:
    SSE: 0.4832
    R-square: 0.9989
    Adjusted R-square: 0.9988
    RMSE: 0.05584
```

Fig. 13 **e** Results of the *cftools* tool of Matlab.

$$S = e = I_{MPP} - I_{PV}$$
$$\dot{S} = \dot{e} = -\dot{I}_{PV} \tag{22}$$

where e is the tracking error. Applying the Lyapunov stability theory, it can be shown that if $\dot{V} < 0$, the value of the switching function (S) tends to zero and therefore the system state converges to MPP.

- When $S > 0$: This implies that the current I_{REF} provided by the reference generator is larger than the current supplied by the module, i.e., $I_{REF} > I_{PV}$ or $I_{MPP} > I_{PV}$. Then, in order to get a zero-tracking error ($S = 0$), I_{PV} must increase and V_{PV} should decrease, which means that R_{PV} has to decrease, achieving this by increasing the duty cycle (d) as can be deduced from Eq. (6). In Fig. 14 it is shown the behavior of the R_{PV}. It can be seen that the system is stable since if I_{PV} increases, then $\dot{S}$ will be negative and also the product $S\dot{S} < 0$, which implies that the system is stable and converges to the maximum power point.
- When $S < 0$: In this case, $I_{PV} > I_{REF}$ or $I_{PV} > I_{MPP}$. Then, in order to get a zero-tracking error ($S = 0$), I_{PV} has to decrease V_{PV} should increase, which means that R_{PV} has to increase, achieving this by decreasing the duty cycle (d) as it can be deduced from Eq. (6). In Fig. 14 it is shown the behavior of the R_{PV}. It can be seen that the system is stable since if I_{PV} decreases, then $\dot{S}$ will be negative and also the product

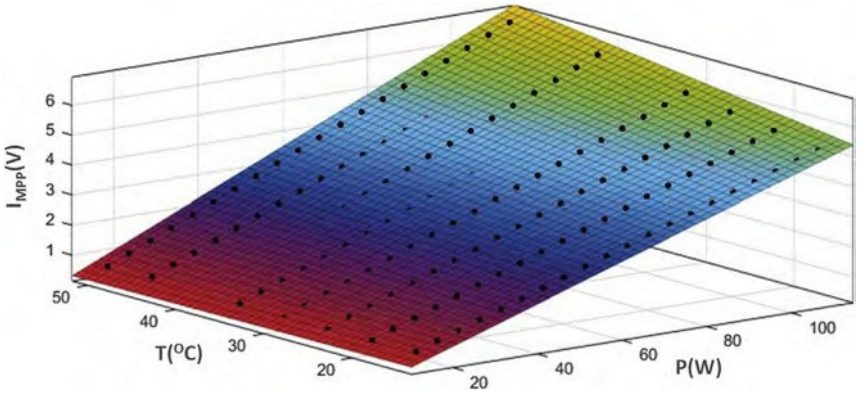

Fig. 12 **e** P-T-I characteristic surface of the MPPs.

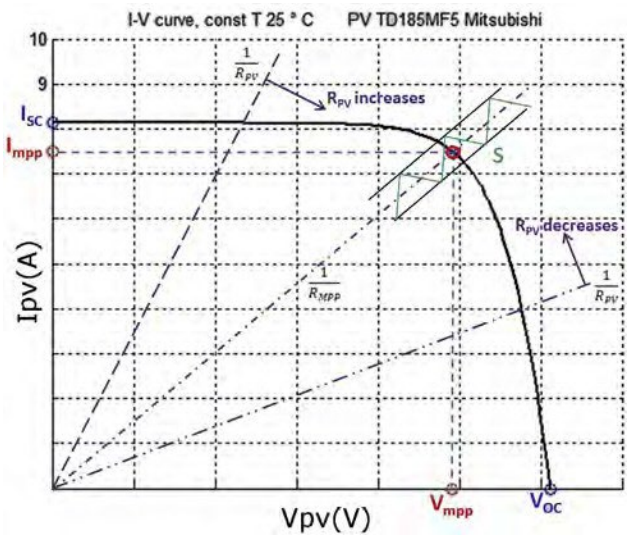

Fig. 14 **e** Influence of the R_{PV} in the I-V characteristic curve.

S:$\dot{S} < 0$, which implies that the system is stable and converges to the maximum power point.

Simulation results of the algorithms

In this section the computer models that simulate our photovoltaic system and have been developed in Matlab/Simulink are introduced. In the simulated models, it is easy to impose arbitrary weather conditions for any experiment. For this reason, in these simulation experiments we will work with four different models, one for each controller, observing their behavior when dealing with sudden variations of temperature and irradiance and analyzing whether they are able to make the photovoltaic module to work at MPP. For this purpose, there are two possibilities: a simulation at constant temperature and variable irradiance, and a simulation at variable temperature and constant irradiance.

In order to know which is the value of the power at the MPP, P**e**I characteristic curves are obtained from the simulated model [18] of the photovoltaic module and the algorithms have run at the temperature and irradiance required for each case. The values obtained are shown in Table 3.

Simulation at constant temperature

The first test is performed at a constant temperature value of 25 °C and with values of irradiance of 600, 700 and 900 W/m² (see Figs. 15).

It is noted that once the output of the four algorithms is stable, they get the same output power than the photovoltaic module (P_{PV}) and that it is the same power value that obtained by the P**e**I characteristic curve of the PV module. There is only a slight variation for the first value of 600 W/m² which can be considered negligible, as shown in Table 3.

The behavior of the four designed control algorithms is very similar, especially for irradiance values of 600 and 700 W/m². In the case of an irradiance of 900 W/m² their behavior is different. The controller that needs more time to stabilize is the implemented through the P&O algorithm as shown in Fig. 17. The second one is the IC algorithm shown in Fig. 16. In the case of the PI controller, it is in the first segment when it needs more time to stabilize, as shown in Fig. 18. The algorithm with the best performance is the sliding mode control, shown in Fig. 19.

Analyzing the behavior of each controller at the converter output, in other words, observing the power that it delivers to the load, it is possible to notice that the behavior of the three controllers is very similar. All of them are able to follow the power of the photovoltaic module with a small power loss due to the converter itself.

Table 3 **e** P_{PV} values obtained at constant temperature and different irradiances.

Temperature 25 °C	600 W/m²	700 W/m²	900 W/m²
P**e**I Curve	79 W	90 W	105 W
Models	78 W	90 W	105 W

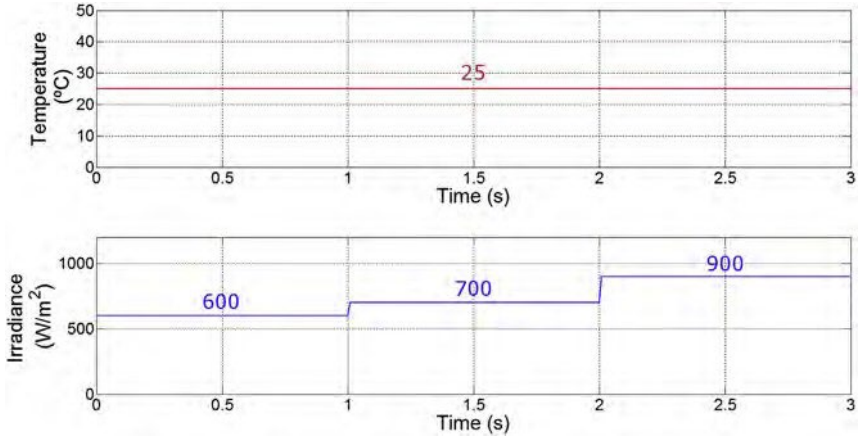

Fig. 15 **e** Temperature (constant) and irradiance (variable) input values.

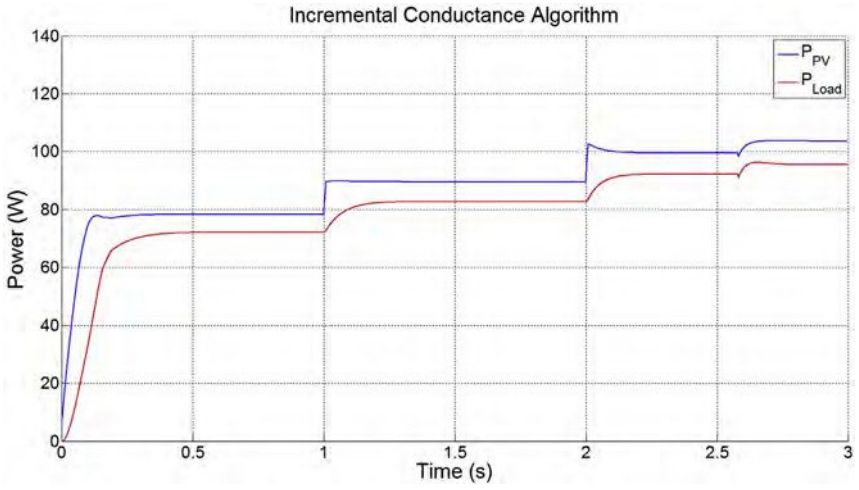

Fig. 16 **e** Power output when sudden irradiance changes using IC algorithm.

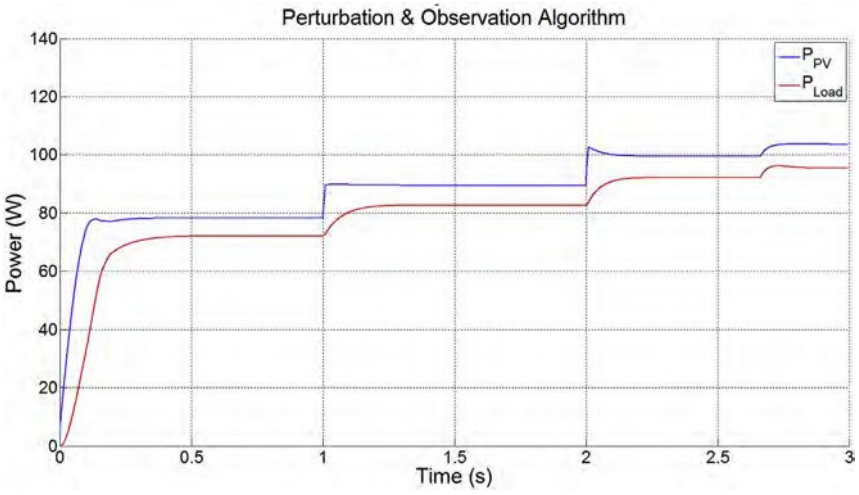

Fig. 17 **e** Power output when sudden irradiance changes using PO algorithm.

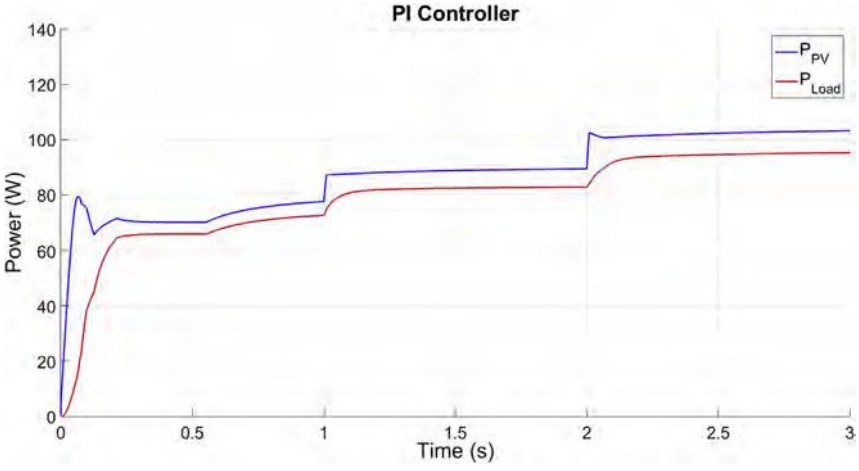

Fig. 18 **e** Power output when sudden irradiance changes using PI controller.

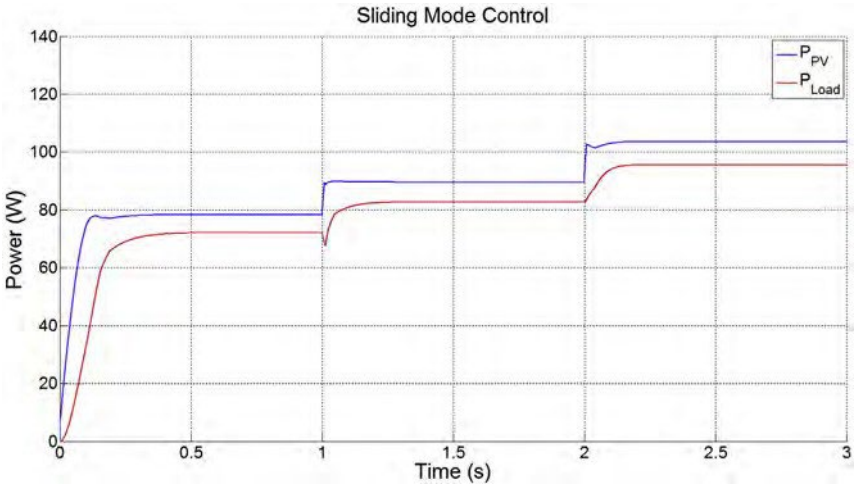

Fig. 19 e Power output when sudden irradiance changes using SMC.

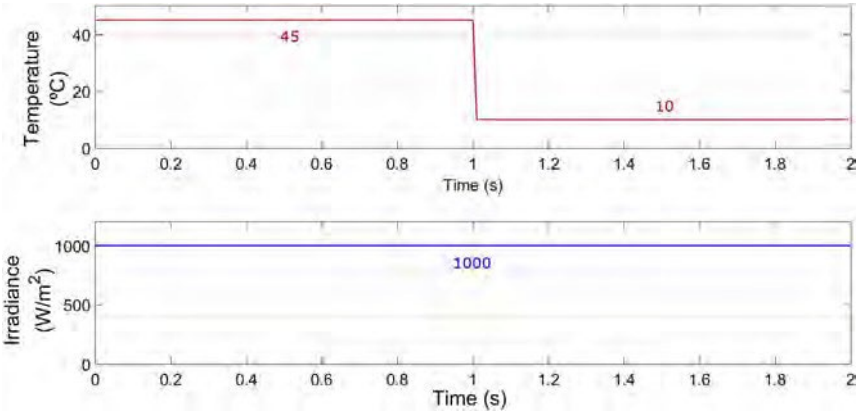

Fig. 20 e Temperature (variable) and irradiance (constant) input values.

Simulation at constant irradiance

In this second test the performance of the algorithms has been analyzed with weather conditions of constant irradiance of 1000 W/m² and temperature values of 45 °C and 10 °C (see Fig. 20).

It is noted that once the outputs are stable, the algorithms achieved an output power of the photovoltaic module (P_{PV}) slightly lower than that obtained using the PeI curves, and even lower for the case of PI controller and the lower temperature, as it is shown in Table 4.

The behavior of the four implemented algorithms is very similar, especially at the higher temperature value. However, in the case of the lower temperature the behavior is different.

Table 4 e P_{PV} values obtained at constant irradiance and different temperatures.

Irradiance 1000 W/m²		
	45 °C	10 °C
PeI Curve	90	120
P&O/IC/SMC	88	117
PI	85	111

The algorithm that needs more time to stabilize is the PI controller (as shown in Fig. 23) followed by P&O (as shown in Fig. 22), and by the IC algorithm (Fig. 21), while the SMC algorithm (Fig. 24) shows a faster stabilization time. So, at the lower temperature the best performance is reached by SMC because is stabilized before, although as was previously mentioned, obtaining less power.

Analyzing the behavior that each algorithm imposes to the converter output, i.e., observing the power delivered to the load, it is noted that the behavior of all of them is very similar in these simulations because they are able to follow the power delivered by the photovoltaic module with a small loss of power due to converter itself, being also in this case the SMC the algorithm that stabilizes the output power in shorter time, while the model based on the PI controller shows the worst behavior.

Real world tests

This section is devoted to assess the performance of the proposed SMC algorithm comparing it with the P&O, IC, PI well known algorithms in real facilities.

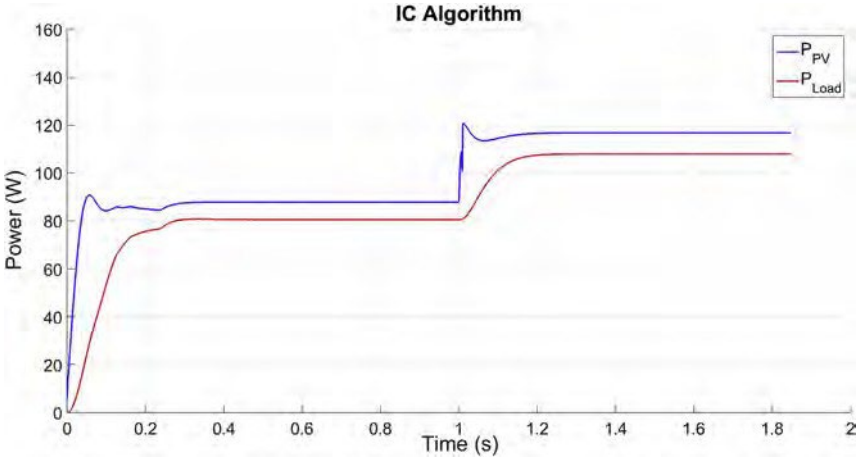

Fig. 21 **e** Power output when sudden temperature changes using IC Algorithm.

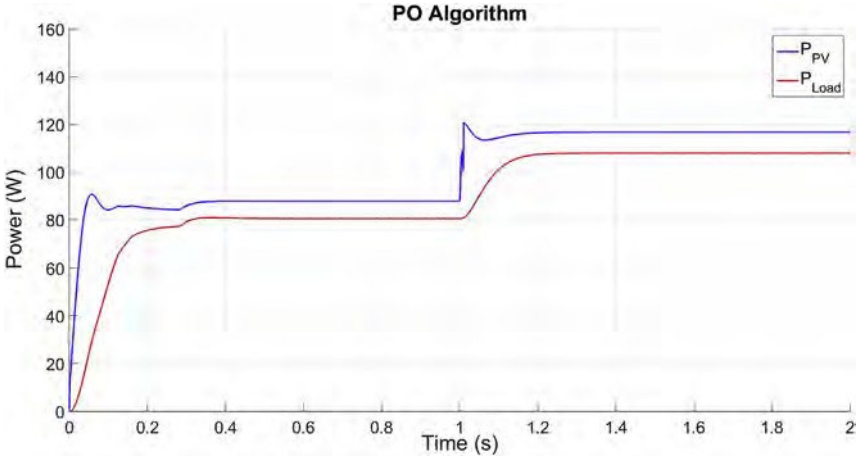

Fig. 22 **e** Power output when sudden temperature changes using PO Algorithm.

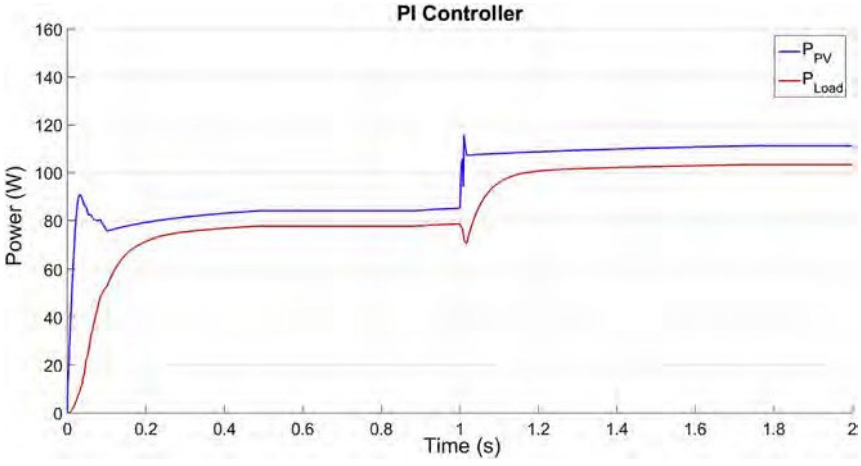

Fig. 23 **e** Power output when sudden temperature changes using PI Controller.

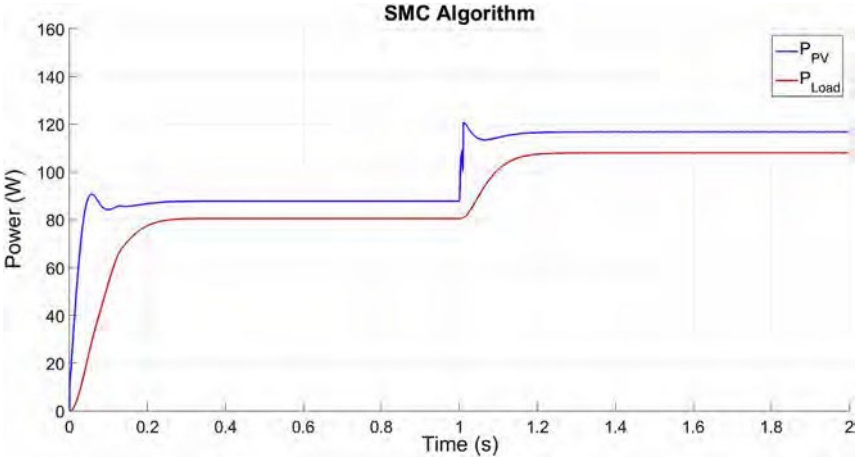

Fig. 24 **e** Power output when sudden temperature changes using SMC.

Experimental setup

The experiments were carried out in one of the laboratories of the Faculty of Engineering Vitoria-Gasteiz (Spain) because the Mitsubishi PV-TD185MF5 photovoltaic modules are located on its roof. The more relevant equipment that has been used during the experiments is the following [10]:

- A boost converter, whose characteristics are shown in Table 5. It has been designed and manufactured by the TEP 192 Research Group of the University of Huelva (Spain).
- A dSPACE DS1104 real-time controller board.
- A variable load from 0 to 400 U.
- A PC for storing the measured data.

In Fig. 25 it is shown a diagram with the most relevant equipment for the experiments and their connections, while Fig. 26 shows the actual elements and the photovoltaic modules used in the real-world tests.

This real-time system allows obtaining values of the system while the control algorithm is running in Matlab/Simulink, as shows Fig. 27. This DSP card is very popular due to its integration capability with Matlab/Simulink through its toolbox in order to work in real time with its real-time interface.

Since these are real world experiments and we need to test the introduced SMC algorithm with real photovoltaic modules, its implementation in Simulink needs to include the following library elements in order to communicate with the DSP board:

Table 5 **e** Boost converter parameters.

Boost converter		
Schottky diode	2xMURF1560GT	600 V, 15 A, 0.4 V 10 A/150 °C
IGBT	1xHGT40N60B3	600 V, 40 A, 1.5 V, 150 °C
L	6xPCV-2-564-08	560 m, 7 A, 42 mU
C	2xTK Series	1500 mF, 250 V

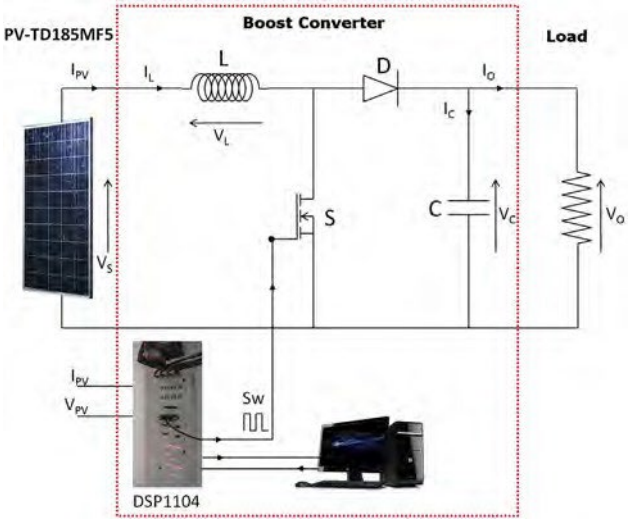

Fig. 25 **e** Main elements of the experimental system and their connections.

- DS1104MUX_ADC: This element is devoted to read up to 4 A/D channels of the converter. Our algorithm needs only to read the irradiance (G) and the temperature (T) at each sampling time.
- DS1104ADC_CX: It is used to read a single channel of the 4 parallel channels of the A/D converter and it is necessary to configure the channel in which we want to read data (from channel ADCH5 to channel ADCH8). In our case ADCH5 reads the photovoltaic generator voltage (V_g ¼ V_{PV}), ADCH6 the photovoltaic generator current (I_g ¼ I_{PV}), ADCH7 the converter output voltage (V_o ¼ V_{LOAD}) and finally, ADCH8 reads the converter output current (I_o ¼ I_{LOAD}).
- DS1104SL_DSP_PWM: It is used to generate standard PWM signals with variable duty cycles and to enable a PWM stop during runtime if needed.

The experiments of the four control algorithms have been carried out in same way: the behavior of the system has been analyzed while controlled by the different control algorithms

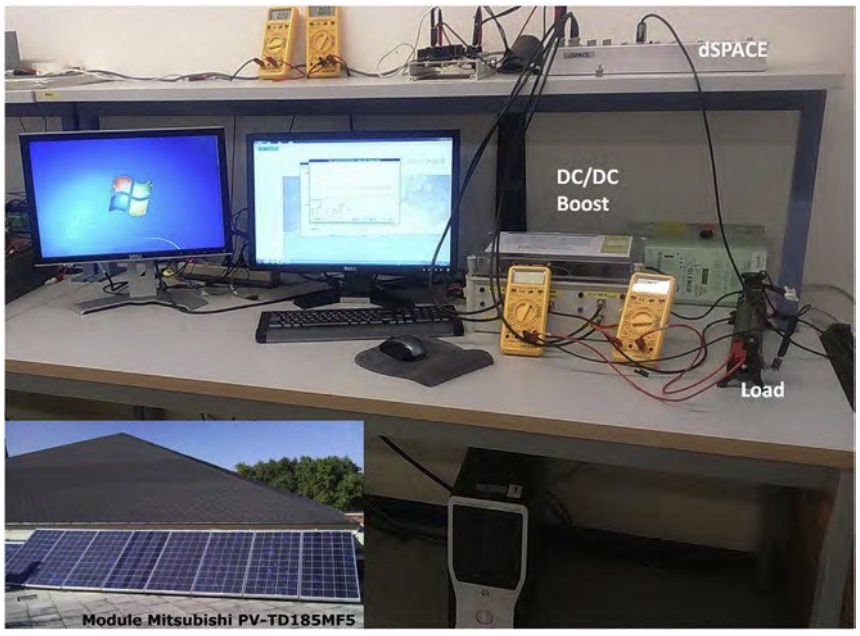

Fig. 26 **e** Actual facilities (laboratory and photovoltaic modules).

when sudden variations in the load between arbitrary values. Besides, we calculated which was the maximum power that should be obtained from the photovoltaic module through its characteristic curves, given the specific weather conditions.

For obtaining the characteristic curves we had several options depending on the used equipment:

- Using the method and equipment as explained in Section Data acquisition: The problem of this method is that there are common elements such as irradiance-temperature sensor and photovoltaic modules that should be disconnected from the scheme of Fig. 9 to be connected to the experimental scheme shown in Fig. 25 spending time in

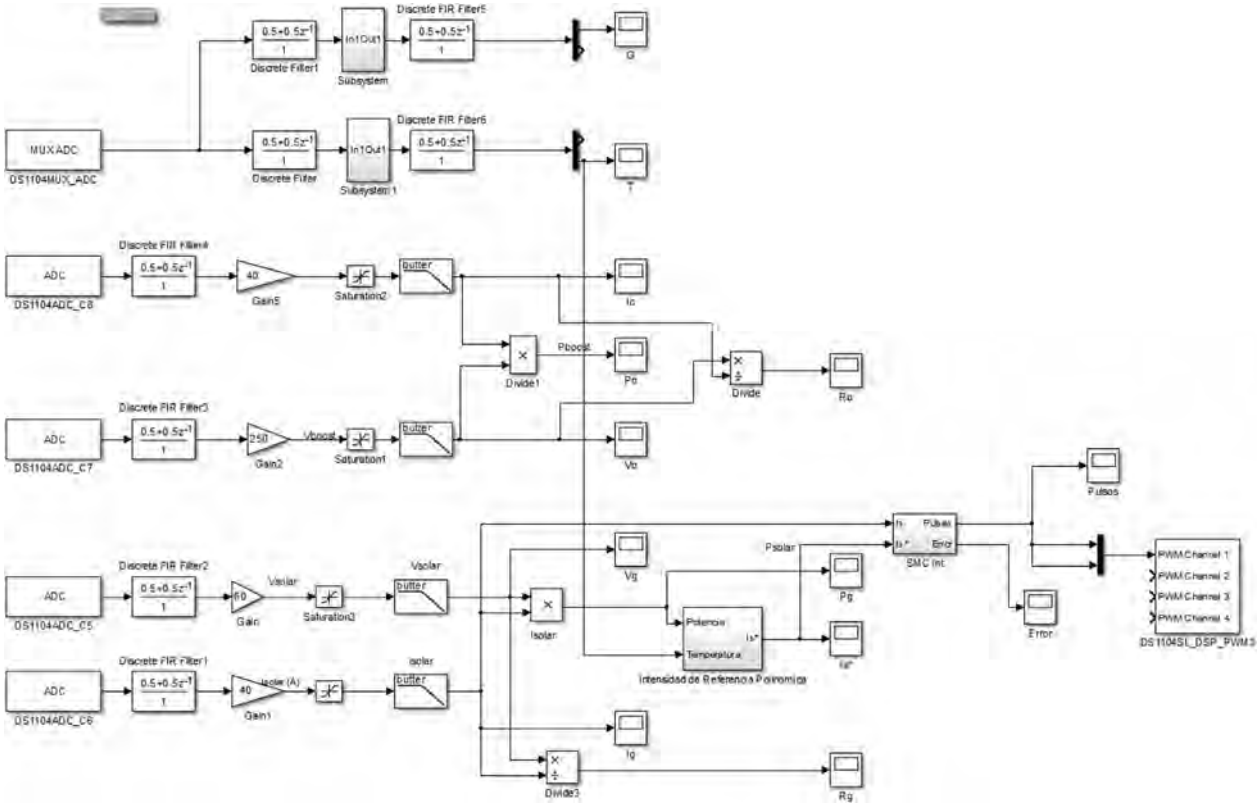

Fig. 27 **e** SMC control algorithm running in Simulink and interacting with the actual photovoltaic module through the DSP.

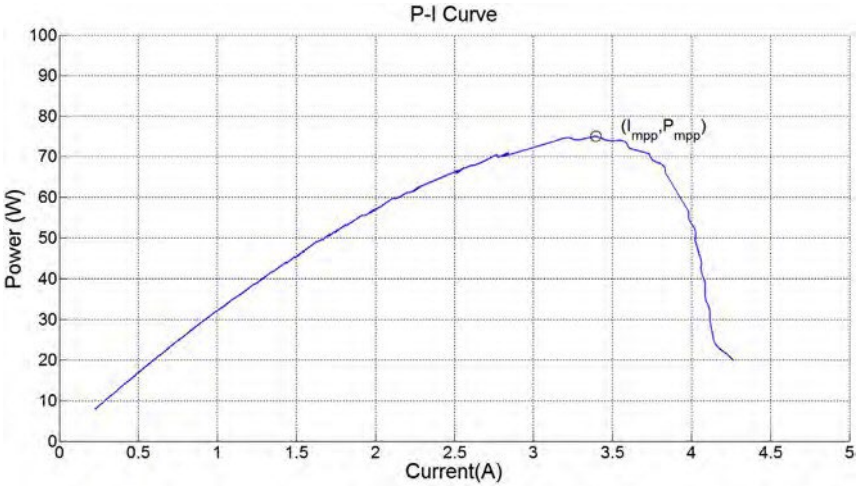

Fig. 28 **e** P-I characteristic curve from experimental data without any control.

this unproductive operation. Besides, when the control measures start again the weather conditions may have changed and the previously obtained characteristics curves would not be useful.

- Using the same equipment of Fig. 25: The first operation to do is to send to DSP a command to make that duty cycle is zero (d ¼ 0) in such a way that the system works without control. The second one is to vary the load from one extreme to the other, i.e., from 0 to 400 U, in such a way that the system goes from the short circuit current (ISC) with R ¼ 0 to close to the open circuit voltage (VOC) with maximum resistance value.
- Using the same equipment of Fig. 25: But in this case the first operation is to send a command to the DSP to make the duty cycle (d) to vary from 0 to 1. The objective is to obtain tuples of current and voltage values to obtain the characteristic curves, along with the existing irradiance and temperature that are also stored. Since it is the fastest method, it is the method that has been used.

Given that these experiments are carried out actual facilities, it is obvious that irradiance and temperature cannot be adjusted to desired values. We have had to adapt to the weather conditions of the days when the experiments were performed. So, we analyze the behavior of the control algorithms with sudden variations in the load values, varying the value of the load resistance placed at the output of converter in an arbitrary way.

Incremental conductance model

The value of the maximum power point of the P**e**I characteristic curve before to be controlled by IC algorithm is 75 W as shown in Fig. 28.

The experiment was carried out with sudden changes in the value of the load resistance R_{Load}: it started with a value of 176 U increasing the value to 307 U, then it is decreased to 139 U and increasing again to 310 U, finishing with a value of 180 U, as shown in Fig. 29.

Regarding the weather conditions during the experiment, it was performed with a temperature of 43 ° C and an irradiance of 794 W/m^2.

The converter makes the photovoltaic module to work supplying a power of approximately 59 W, as shown in Fig. 30.

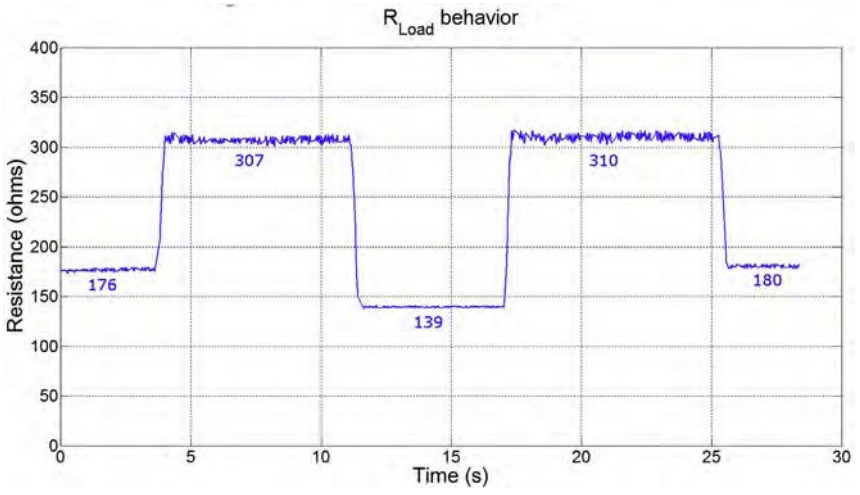

Fig. 29 **e** Changes in the load resistance R_{Load} during the IC control real experiment.

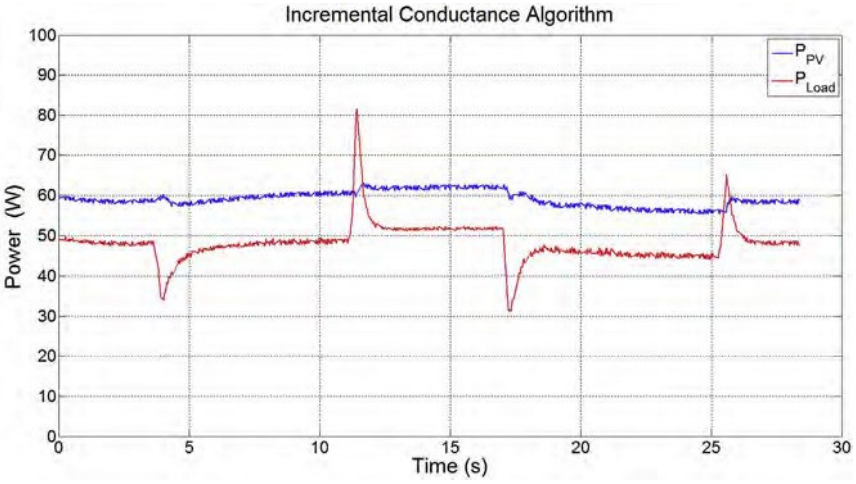

Fig. 30 **e** Real behavior of P_{PV} and P_{Load} when using IC algorithm.

This implies that the control algorithm cannot reach the MPP shown by the characteristic curve. So, we have assessed that although the behavior of this algorithm is globally correct, it does not exhibit a good performance in power terms.

Perturbation and observation algorithm

The value of the maximum power point of the P**e**I characteristic curve before to be controlled by P&O algorithm is 67.77 W, as shown in Fig. 31.

The experiment was carried out with sudden changes in the value of the load resistance R_{Load}: it started with a value of 319 U decreasing the value to 220 U, then it was increased to
339 U and decreased again to 276 U, and finally it was increased to 350 U and finished with a value of 277 U, as shown in Fig. 32.

This second experiment was carried out with weather conditions of temperature of 45 °C and irradiance of approximately 700 W/m².

The converter is able of make the photovoltaic module to work at a power of 69 W, i.e., very close to the maximum power value indicated by the characteristic curve, assuming that the weather conditions during the experiment vary somewhat because it takes a while since the values of the characteristic curve are obtained until the control behavior is analyzed, as shown in Fig. 33.

The behavior of the output power of the panel (P_{PV}) could be acceptable if the load resistance would be at values superior to 220 U. We see that when the load has this value the power decreases. The module is not able to work well at that power. The algorithm shows slight oscillations but it maintains the output power of the module at a power close to maximum power point.

PI controller algorithm

The value of the maximum power point of the P**e**I characteristic curve before to be controlled by PI controller is 41.74 W, as shown in Fig. 34.

The experiment was carried out with sudden changes in the value of the load resistance R_{Load}: it started with a value of 161 U increasing it up to 325 U, then it was decreased to 85 U to

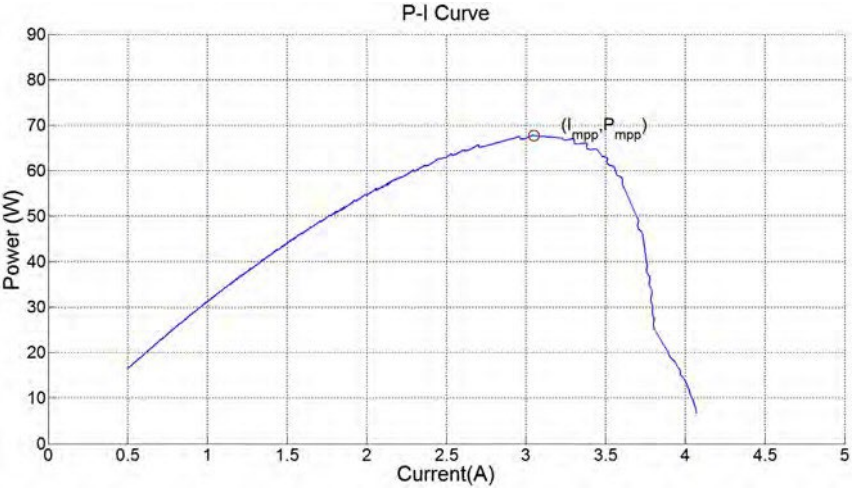

Fig. 31 **e** P-I characteristic curve from experimental data without any control.

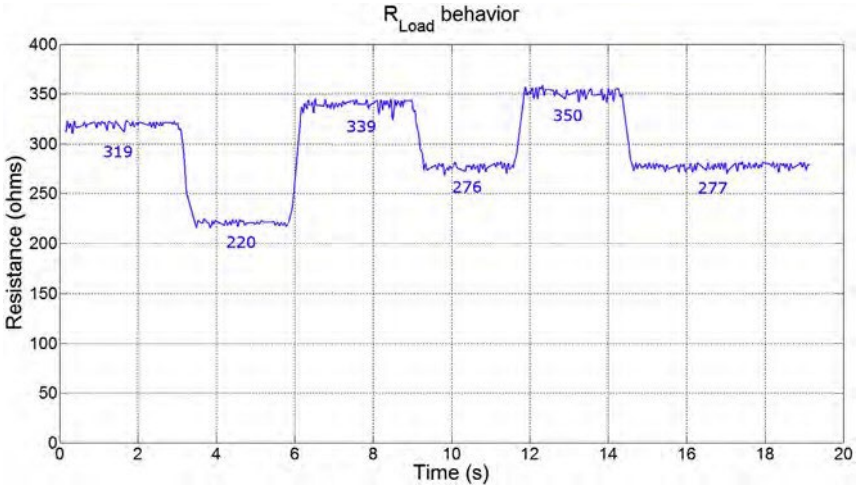

Fig. 32 **e** Changes in the load resistance R_{Load} during the PO control real experiment.

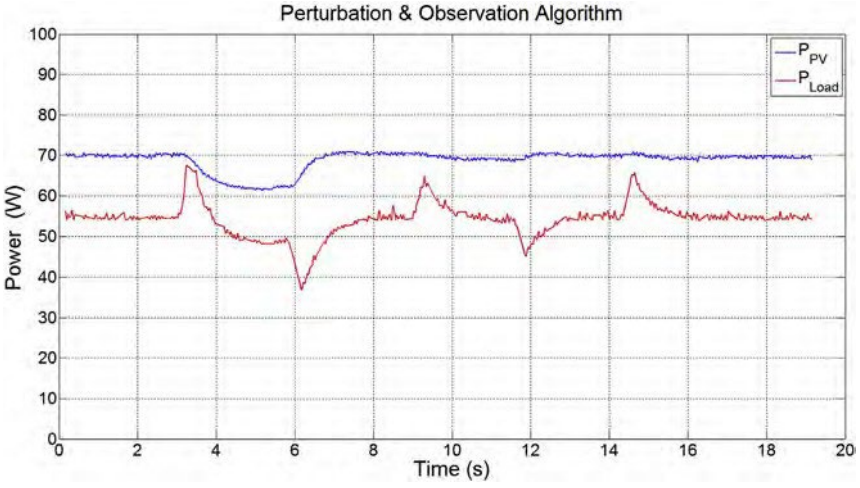

Fig. 33 **e** Real behavior of P_{PV} and P_{Load} when using P&O algorithm.

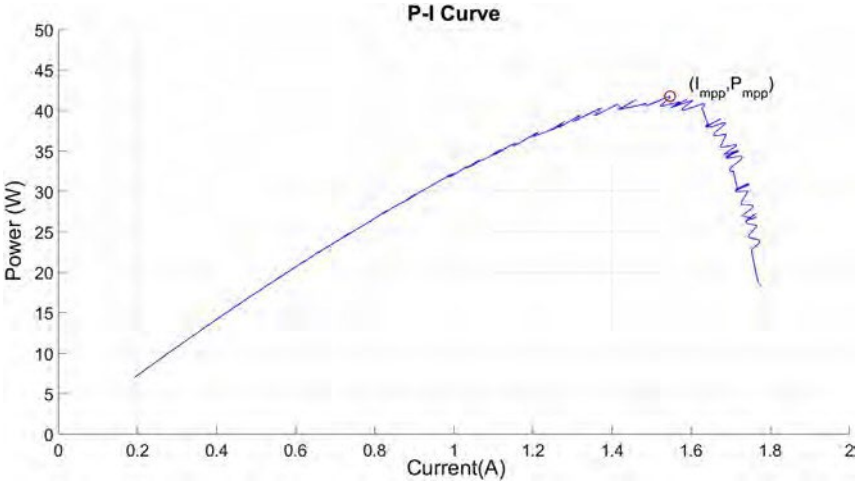

Fig. 34 **e** P-I characteristic curve from experimental data without any control.

finish the experiment with a value of the load resistance of 325 U, as we can see in Fig. 35.

The behavior of the voltage and current at the output of the photovoltaic module is shown in Fig. 36. In the case of the voltage it is observed that it has a very oscillating behavior, especially with the values of smaller resistances.

After analyzing the behavior of the voltage and of the current at the output of the photovoltaic module (V_{PV} and I_{PV}), it is observed that the behavior of the output power P_{PV} at module terminals is acceptable. Although it is observed that the voltage has noise, it is not transferred to the power signal because when it is multiplied by the current that noise is compensated, as seen in Fig. 37.

Sliding mode control algorithm

The value of the maximum power point of the P**e**I characteristic curve before to be controlled by SMC based algorithm is 72.47 W, as shown in Fig. 38.

As in previous ones, this experiment was carried out applying sudden changes in the value of the load resistance. The experiment started with a value of R_{Load} equal to 260 U increasing it up to 347 U, then it is decreased until 226 U to finish the experiment with a value of the load resistance of 333 U, as we can see in Fig. 39.

This last experiment was carried out with weather conditions of 57 ° C of temperature and an irradiance of approximately 890 W/m^2.

In Fig. 40 we can analyze the behavior of the reference current (I_s*) which is given by the current reference generator and the current at the output of the photovoltaic module (I_{PV}), obtaining mean values of 4.5137 A for I_{REF} and 4.5112 A for I_{PV}. The photovoltaic module current follows continuously the reference current even when the load resistance has sudden variations.

Fig. 41 shows the behavior of the voltage (in blue) and the current (in red) at the output of the photovoltaic module, being both magnitudes very stable. The current (I_{PV}) obtained a mean value of 4.5137 A, while the voltage (V_{PV}) obtained a mean value of 16.40 V.

We can see in Fig. 42 that the PV module has been working at a power (73.9 W) very close to the maximum power value that indicates the corresponding characteristic curve, given that the weather conditions may vary somewhat because it takes a while since the values of the characteristic curve are obtained until the control behavior is analyzed.

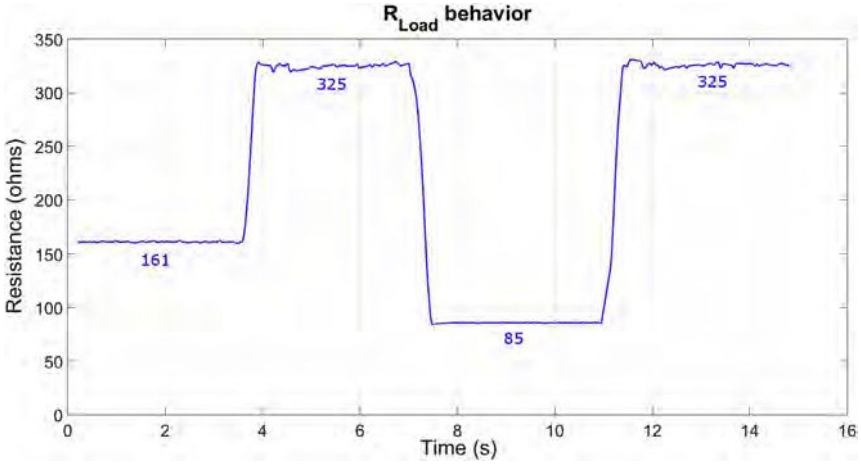

Fig. 35 **e** Changes in the load resistance R_{Load} during the PI control real experiment.

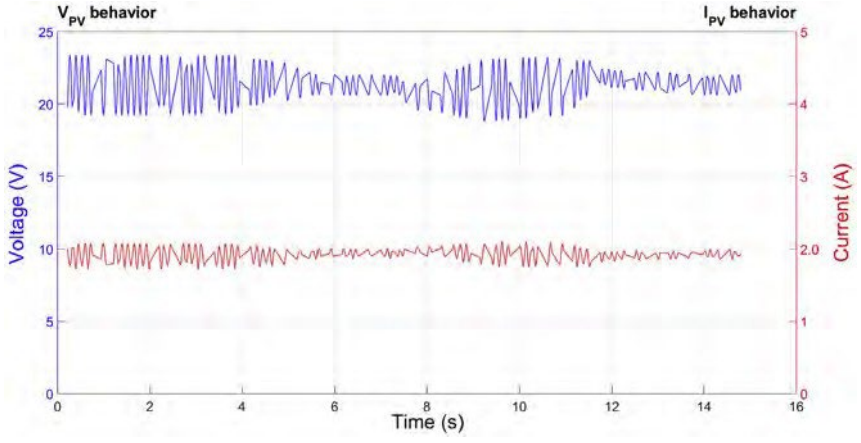

Fig. 36 **e** Real behavior of V_{PV} and I_{PV} when using PI controller.

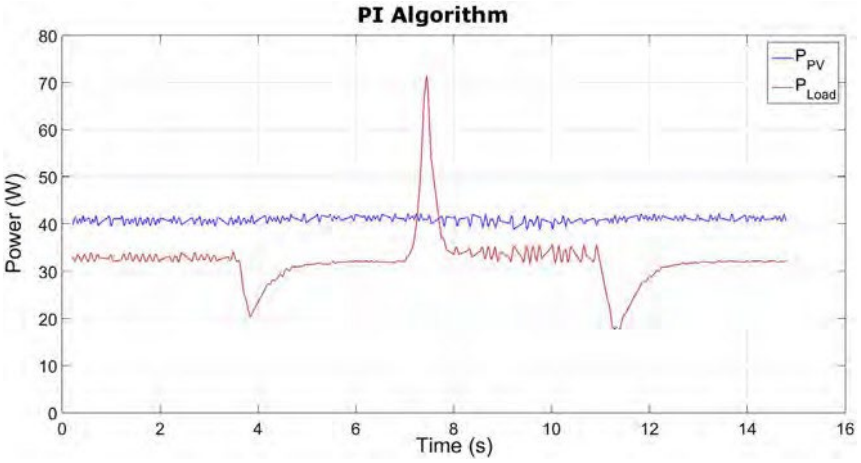

Fig. 37 **e** Real behavior of P_{PV} and P_{Load} when using PI controller.

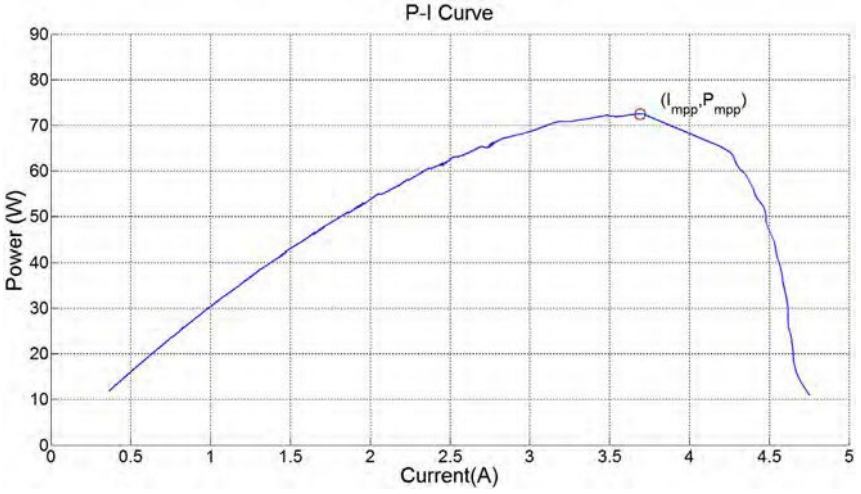

Fig. 38 **e** P-I characteristic curve from experimental data without any control.

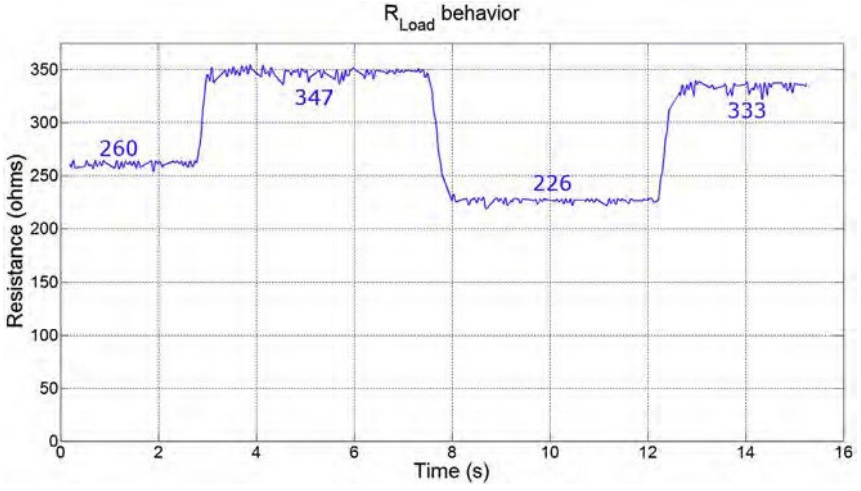

Fig. 39 **e** Changes in the load resistance R_{Load} during the SMC control real experiment.

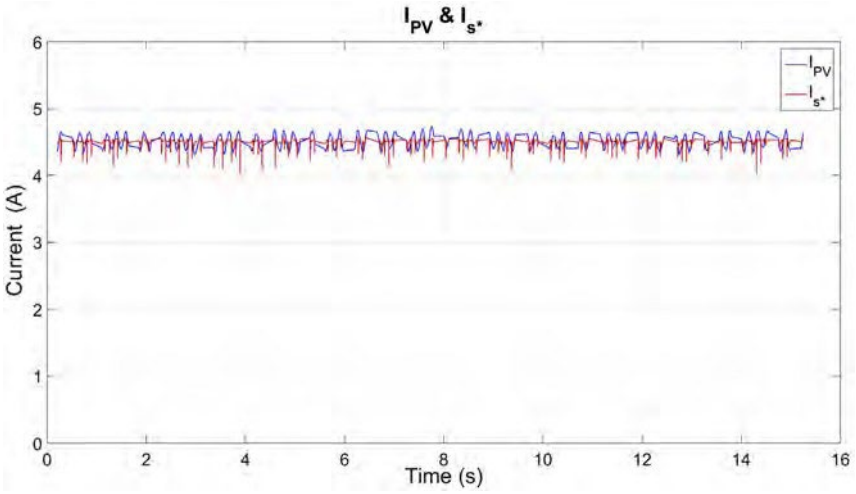

Fig. 40 **e** Real behavior of I_S* and I_{PV} when using SMC based algorithm.

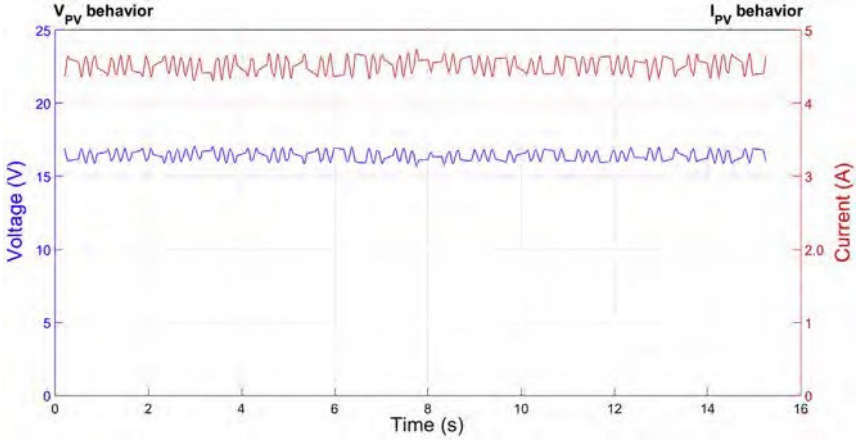

Fig. 41 **e** Real behavior of V_{PV} and I_{PV} when using SMC algorithm.

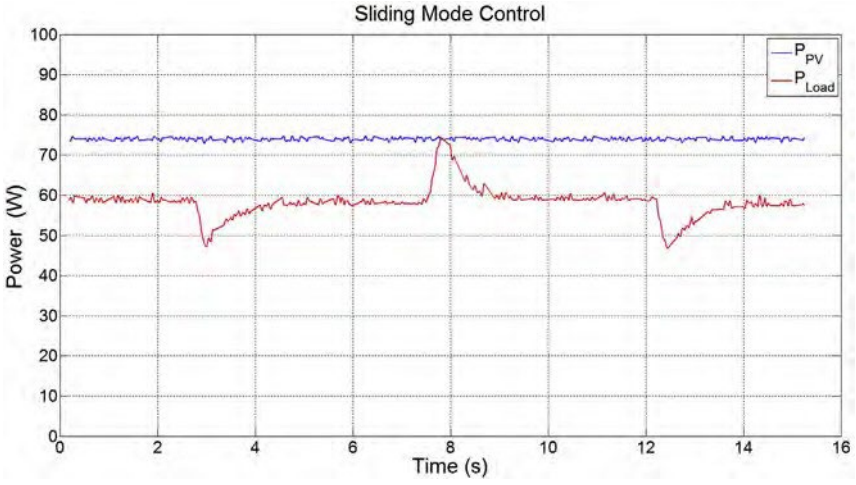

Fig. 42 **e** Real behavior of P_{PV} and P_{Load} when using SMC algorithm.

In this case, the power obtained from the module photovoltaic is much more linear that in the other three experiments because the changes of the load resistance have no influence. So, we state that this one is the best of the four control algorithms because it makes the photovoltaic module to work in the MPP regardless of load variations.

Conclusion

In this paper authors introduce a novel sliding mode control for maximum power point tracking (MPPT). As part of that novel SMC algorithm, a reference current generator is designed based on a set of data collected during 20 months by the authors.

The first part of the paper describes the problem addressed in this paper and gives a complete background on some topics related to the problem to solve. Then the novel design of the SMC control is described in detail.

In order to assess its design, the novel control is compared with three of the most commonly used control algorithms in the scope of MPP tracking in photovoltaic energy and in industry. The purpose of the comparison of these four control algorithms is to test the improvement of the performance of the photovoltaic module, paying attention to the generated output power and its similarity to the MPP.

The first part of the comparison is carried out in a simulated environment, were the four controls have shown a very similarly performance when dealing with sudden variations of irradiance and constant temperature and vice versa, i.e., with constant irradiance values and abrupt temperature variations.

In the second part of the comparison, the four algorithms are compared when working in real time in a facility located at the Faculty of Engineering Vitoria-Gasteiz. In this case their response is analyzed when there are sudden variations in the value of the load resistance placed at the output of the DC/DC converter. The four control algorithms have been developed in the Matlab-Simulink environment with a dSPACE DS1104 card for real-time interaction with the real photovoltaic module. In this case the best results have been obtained by the proposed SMC based algorithm. One of its more outstanding advantages is that it has a simple implementation but it can obtain very good results, with a high precision in the MPP tracking task. Besides, the proposed SMC algorithm ensures the stability of the installation as well as its efficiency, improving the behavior of the photovoltaic module when compared to the other three control algorithms.

Acknowledgments

The authors are very grateful to the UPV/EHU for its support through Projects GIU13/41 and UFI11/07. The authors are also grateful to European Union Ministry of Turkey, National Agency of Turkey for the support of this project under the Project Code: 2015-1-TR01-KA203-021342 entitled Innovative European Studies on Renewable Energy Systems.

[1] Alajmi BN, Ahmed KH, Finney SJ, Williams BW. Fuzzy-logic-control approach of a modified hill-climbing method for maximum power point in microgrid standalone photovoltaic system. IEEE Trans Power Electron 2011;26(4):1022e30.

[2] Algazar MM, AL-Monier H, EL-Halim HA, El Kotb Salem ME. Maximum power point tracking using fuzzy logic control. Int J Electr Power & Energy Syst 2012;39(1):21e8.

[3] Alqahtani AH, Utkin VI. Self-optimization of photovoltaic system power generation based on sliding mode control. In: 16 International Journal of Photoenergy in proceedings of the 38th annual conference on IEEE industrial electronics society (IECON '12). Montreal, Canada: IEEE; October 2012. p. 3468e74.

[4] Andújar JM, Barragán AJ, Gegúndez ME, Maestre M. Control Borroso Multivariable Basado en Heurı´stica. Un Caso Práctico: grúa Porta Contenedores. Rev Iberoam Automática Inform Ind 2007;4(2):81e9.

[5] Cid-Pastor A, Martinez-Salamero L, El Aroudi A, Giral R, Calvente J, Leyva R. "Synthesis of loss-free resistors based on sliding-mode control and its applications in power processing". Control Eng Pract 2013;21(5):689e99.

[6] Guilbert Damien, Gaillard Arnaud, Mohammadi Ali, N'Diaye Abdoul, Djerdir Abdesslem. Investigation of the interactions between proton exchange membrane fuel cell and interleaved DC/DC boost converter in case of power switch faults. Int J Hydrogen Energy 5 January 2015;40(1). ISSN: 0360-3199:519e37. http://dx.doi.org/10.1016/j.ijhydene.2014.10.072.

[7] Drissi H, Khediri J, Zaafrane W, Ben Braiek E. Critical factors affecting the photovoltaic characteristic and comparative study between two maximum power point tracking algorithms. Int J Hydrogen Energy 2017;42:8689e702.

[8] Elmetennani S, Laleg-Kirati TM, Djemai M, Tadjine M. New MPPT algorithm for PV applications based on hybrid dynamical approach. J Process Control 2016;48:14e24.

[9] Esram T, Chapman PL. Comparison of photovoltaic array maximum power point tracking techniques. IEEE Trans Energy Convers EC 2007;22(2):439.

[10] Farhat M, Barambones O, Ramos-Hernanz JA, Duran E, Andujar JM. Diseño e Implementación de un Sistema de Control estable basado en Lógica Borrosa para optimizar el rendimiento de un sistema de Generación Fotovoltaico. Rev Iberoam Automática Inform Ind RIAI 2015;12(4):476e87.

[11] Fazel T, Zainal S, Shahrin MA. FPGA implementation of a single-input fuzzy logic controller for boost converter with the absence of an external analog-to-digital converter. IEEE Trans industrial Electron 2012;59(2):1208e17.

[12] Marzooghi H, Raoofat M. Improving the performance of proton exchange membrane and solid oxide fuel cells under voltage flicker using Fuzzy-PI controller. Int J Hydrogen Energy May 2012;37(9). ISSN: 0360-3199:7796e806. http://dx.doi.org/10.1016/j.ijhydene.2012.01.130.

[13] Hirosato S. Nonlinear identification using single input connected fuzzy inference model. In: 17th International conference in knowledge based and Intelligent Information and engineering systems; 2013.

[14] Houssamo I, Locment F, Sechilariu M. Maximum power tracking for photovoltaic power system: development and experimental comparison of two algorithms. Renew Energy 2010;35(10):2381e7.

[15] Kilkis B. District energy systems: theory and applications. J Polytech 2011;14(2):149e54.

[16] Levron Y, Shmilovitz D. Maximum power point tracking employing sliding mode control. IEEE Trans Circuits Syst I Regul Pap 2013;60(3):724e32.
[17] Logeswaran T, SenthilKumar A. A review of maximum power point tracking algorithms for photovoltaic systems under uniform and non-uniform irradiances. Energy Procedia 2014;54:228e35.
[18] Lopez-Guede JM, Ramos-Hernanz JA, Zulueta E, Fernandez-Gamiz U, Oterino F. Systematic modeling of photovoltaic modules based on artificial neural networks. Int J Hydrogen Energy 2016;41(29). ISSN: 0360-3199:12672e87. http://dx.doi.org/10.1016/j.ijhydene.2016.04.175. 3 August 2016.
[19] Noman AM, Addoweesh KE, Mashaly HM. DSPACE real-time implementation of MPPT-based FLC method. Int J Photoenergy 2013;2013.
[20] Park J, Kim S. Maximum power point tracking controller for thermoelectric generators with peak gain control of boost DCeDC converters. J Electron Mater 2012;41(6):1242e6.
[21] Purushothaman G, Venugopalan V, Vincent AM. Real-time simulation platform for photovoltaic system with a boost converter using MPPT algorithm in a DSP controller. Front Energy 2013;7(3):373e9.
[22] Saadi R, Kraa O, Ayad MY, Becherif M, Ghodbane H, Bahri M, et al. Dual loop controllers using PI, sliding mode and flatness controls applied to low voltage converters for fuel cell applications. Int J Hydrogen Energy 9 November 2016;41(42). ISSN: 0360-3199:19154e63. http://dx.doi.org/10.1016/j.ijhydene.2016.08.171.
[23] Rezk H, Eltamaly AM. A comprehensive comparison of different MPPT techniques for photovoltaic systems. Sol Energy 2015;112:1e11.
[24] Salas V, Olías E, Barrado A, Lázaro A. Review of the maximum power point tracking algorithms for stand-alone photovoltaic systems. Sol Energy Mater Sol Cells 2006;90(11):1555e78.
[25] Sawant JV, Ginoya DL. dSPACE DS1104 based proportional integral sliding mode controller for continuous conduction mode buck boost converter. In: 14th dSPACE user conf; 2012.
[26] Shotorbani AM, Gassemzadeh S, Mahboubi B. Design and comparison of a novel controller based on control Lyapunov function and a new sliding mode controller for robust power flow control using UPFC. Gazi Univ J of Sci 2014;27(1):679e92.
[27] Singh P, Palwalia DK, Gupta A, Kumar P. Comparison of photovoltaic array maximum power point tracking techniques. Int Adv Res J Sci Eng Technol 2015;2(1).
[28] Sivakumar P, Kader AA, Kaliavaradhan Y, Arutchelvi M. Analysis and enhancement of PV efficiency with incremental conductance MPPT technique under non-linear loading conditions. Renew Energy 2015;81:543e50.
[29] Soufi Y, Bechouat M, Kahla S. Fuzzy-PSO controller design for maximum power point tracking in photovoltaic system. Int J Hydrogen Energy 2017;42:8680e8.
[30] Sundareswaran K, Palani S. Application of a combined particle swarm optimization and perturb and observe method for MPPT in PV systems under partial shading conditions. Renew Energy 2015;75:308e17.
[31] Tafticht T, Agbossou K, Doumbia ML, Cheriti A. An improved maximum power point tracking method for photovoltaic systems. Renew energy 2008;33(7):1508e16.
[32] Tavana MR, Khooban MH, Niknam T. Adaptive PI controller to voltage regulation in power systems: STATCOM as a case study. ISA Trans 2016. http://dx.doi.org/10.1016/j.isatra.2016.09.027i.
[33] Villalva MG, Gazoli JR, Ruppert Filho E. Analysis and simulation of the P&O MPPT algorithm using a linearized PV array model. 35 IECON'09. 2009.
[34] Zhang F, Maddy J, Premier G, Guwy A. Novel current sensing photovoltaic maximum power point tracking based on sliding mode control strategy. Sol Energy 2015;118:80e6.